Ten Noorden van de Waddeneilanden Field Measurement Campaign

Validation Report - January 2021

Deltares

Ten Noorden van de Waddeneilanden Field Measurement Campaign

Validation Report - January 2021

Sofia Caires

11203488

Deltares

Title
Ten Noorden van de Waddeneilanden Field Measurement Campaign

Client	Project	Reference	Pages
Fugro	11203488	11203488-002-HYE-0002	58

Classification
None

Keywords
North Sea, wind farm, metocean data, validation, offshore wind

Summary
Two *SEAWATCH Wind LiDAR Buoys*, TNWA and TNWB, have been deployed by Fugro at the Ten Noorden van de Waddeneilanden Wind Farm Zone on the 19th of June 2019, with the intention of measuring wind, waves, temperatures, pressures and currents for a period of two years. In order to also collect bottom temperature and water level data, two bottom mounted sensors have then also been deployed near TNWA and TNWB. Because the mooring at TNWA become unusable, on the 16th of January 2021 an additional station TNWA-2 (a new mooring location, close to the initial TNWA location) was added. The redundant arrangement of instruments is intended to safeguard against loss in measured data. In order to further avoid gaps in the data, there has been some servicing and swapping of the buoys and sensors when needed.

In this report the validation of the measurements during January 2021 is presented.

Because the buoy has only been deployed on the 16th, the availability of all data from TNWA-2 is poor. Unfortunately, the availability of current, water level and bottom temperature data from TNWB is also poor. On the other hand, the availability of wave, air pressure and air and surface water temperature data from TNWB is high. The availability of wind data from TNWB is also high, except for the LiDAR wind direction data which is acceptable, with most of the data missing after the 26th of January when data from TNWA-2 are available.

The validation of the available data is performed by intercomparing the TNWA-2 and TNWB observations and validating against wind, waves, air and water temperature, air pressure, water level and currents from a variety of reliable sources (anemometer, LiDAR, hydrodynamic model, etc) at reference stations in the North Sea; namely L91, K13, F3, AWG, HG, SON and BG.

The following conclusions ensue from the validation of the data.
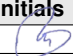
- The comparisons between the TNWA-2 and TNWB wind velocities show at all levels and in terms of both wind speed and direction low biases and correlations and slopes close to 1, indicating correct functioning of both LiDARs. Furthermore, the validation of the TNW data against the observations from the fixed stations and model data, show that mismatches can be explained by local effects and spatial and vertical variations.
- The agreement between the TNWA-2 and TNWB wave parameters is excellent for all parameters, except in terms of swell mean wave period which is good, peak wave period which is reasonable and mean wave direction which is poor. The poorer agreements are as expected, given that these parameters depend more strongly on the sampling variability (randomness of the sea surface elevation) and discreteness of the wave spectra. The agreement between the wave observations from TNW and from the reference stations is relatively high, especially when considering local refraction and the distances between the stations.

- The validation of the temperature data shows that there are large spatial variations in the water temperatures during this period and a general agreement between TNW and fixed station air temperature observations.
- The validation of the air pressure data shows, as expected given their proximity in terms of macro-atmospheric forcings, an excellent agreement between the TNW observations and those from the fixed stations.
- Even though the water level data availability, in particular from TNWB, is low, there is a high correlation between the model and the available TNW water levels, testifying to the quality of both the TNW and the model data.
- The agreement between the current speed observations and model results is high. There are mismatches between the current directions, which are partly due to the nature and variability of the current direction signal.

The overall conclusion of the validation is that the available TNW data are of high quality and trustworthy.

References
None

Version	Date	Author	Initials	Review	Initials	Approval	Initials
1.0	Apr. 19, 2021	S. Caires		J. Schouten		M. van Gent	

Status
Final

Contents

Deltares

List of Figures

Deltares

Deltares

Deltares

List of Tables

Deltares

1 Introduction

Aiming at high collection rates of quality metocean data, two *SEAWATCH Wind LiDAR Buoys* were deployed by Fugro at the Ten Noorden van de Waddeneilanden Wind Farm Zone. The two buoys are referred to as Station A and Station B but are abbreviated in this report as TNWA and TNWB, respectively. Additionally, bottom mounted water level sensors (WLS) have been deployed near the buoys. The deployment date is the 19th of June 2019, when buoy WS190 was deployed at TNWA and buoy WS191 deployed at TNWB. The campaign aims at measuring wind, waves, temperatures, pressures and currents for a period of two years.

The redundant arrangement of instruments is intended to safeguard against loss in measured data. This is an efficient approach given that it has led to an almost continuous data record per variable from TNW in spite of a few problems. Unfortunately, often problems can only be solved by going to the site and servicing or replacing the buoys. In the following the issues and deployment and recovery events that have led to relevant data gaps are listed. The full record of issues is given in the report of Fugro accompanying the data.

- Communication with the WLS at TNWA failed right after deployment in June 2019.
- Connection was lost with the LiDAR at TNWB from the 12th of September 2019 until the 23rd of January 2020, when the buoy was serviced and the data downloaded.
- The LiDARs on both buoys stopped working at the end of December 2019.
- On the 22nd of January 2020 buoy WS190 was swapped with buoy WS170 at TNWA and buoy WS191 at TNWB removed. With no TNWB buoy and WLS data being available from this date. Due to weather constrains it was not possible to deploy a buoy at TNWB until April 2020.
- On the 11th of April buoy WS170 was recovered and buoy WS190 deployed at TNWA and buoy WS191 deployed at TNWB. From this time WLS observations from both TNWA and TNWB are available.
- Because of performance problems with the LiDAR at WS191, on the 24th of June 2020 buoy WS191 was swapped with buoy WS170 at TNWB.
- Again due to LiDAR performance issues, there was a swap of buoy WS190 with buoy WS191 at TNWA (same mooring) on the 22nd of July 2020.
- On the 14th of September 2020 buoy WS170 was swapped with buoy WS190 at TNWB.
- At 11:20 on the 25th of October 2020 buoy WS190 started drifting, with no data being available from TNWB from this date until 07:40 on the 10th of November 2020 when buoy WS156 was deployed at TNWB.
- At 11:30 on the 30th of December 2020 buoy WS191 at TNWA began to drift and data are missing from that point onwards.
- Because after the drift of WS191 from TNWA there were parts of the mooring left at TNWA, an additional station TNWA-2 was added a bit farther away and buoy WS199 deployed there on the 16th of January 2021.
- On the 25th of January 2021 buoy WS156 was swapped with buoy WS187 at TNWB.

Information regarding the approximate location of the buoys during this reporting period is given in Table 1.1. As the WLS have been deployed close to the buoy, its coordinates are assumed to coincide with those of the buoy. The bathymetry around the approximate location of the buoys is shown in Figure 1.1.

Table 1.1: *Ten Noorden van de Waddeneilanden LiDAR Buoy mooring locations and hull numbers (January 2021).*

Station	Hull number	Longitude (E)	Latitude (N)	Depth (mMSL)
TNWA	None	5.5502°	54.0181°	≈ 38
TNWA-2	WS199 (from 2021-01-16 08:40)	5.5638°	54.0182°	≈ 38
TNWB	WS156 (until 2021-01-25 09:10)	5.5498°	54.0218°	≈ 38
TNWB	WS187 (from 2021-01-25 10:20)	5.5498°	54.0218°	≈ 38
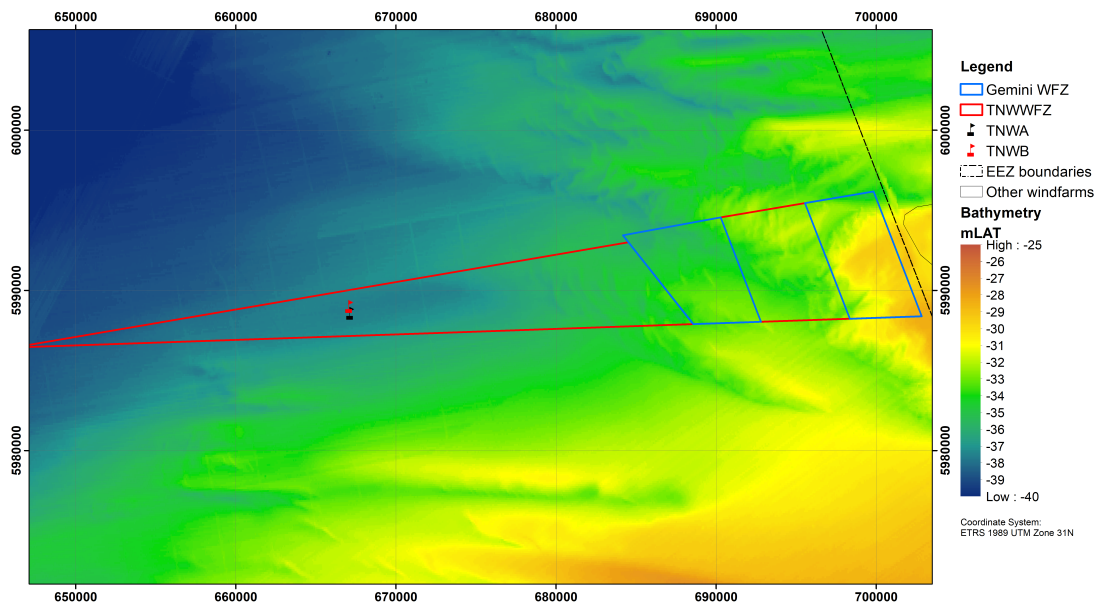
Figure 1.1: *Bathymetry (mLAT, mLAT≈ -1 mMSL) around the buoy locations.*

The main aim of this report is to provide an overview and validation of the TNW post-processed wind, wave, temperature, air pressure, water level and current observations, mainly focusing on the validation of the wind, wave and current data. The assessment of the integrity of the buoy data processing and the quality of the pre-processed data are outside the scope of the validation. The validation is carried out by quantifying the agreement between the TNWA-2 and TNWB data, indicating correct functioning of the different sensors without loss of accuracy, and data from other reliable sources (anemometer, LiDAR, atmospheric model, hydrodynamic model, etc) at fixed North Sea reference stations (no temporary campaigns). If the same variations are found in the parameters, this can be seen as an indication that both buoy systems are functioning correctly with no system errors in the measurements. Furthermore, for some variables their general characteristics are also qualitatively assessed, such as for current and wind measurements their respective vertical profiles. Per variable the most suitable available data validation sources have been sought, leading to the following combinations:

- The reference stations for validating the buoy wind data against anemometer observations are those from platform L91 (where the anemometer is at height z=87 m), referred to as L91, platform K13 (z=73.8 m), referred to as K13, platform Ameland Westgat (z=60 m), referred to as AWG and those from the Huibergat station (z=18 m), referred to as HG. These stations are approximately at a distance of respectively 59 km (L91), 178 km (K13), 64 km (AWG) and 75 km (HG) from the TNW buoys. Data from F3 (z=60 m, distance=107 km) have also been considered, but there are no valid wind observations from the station during this period. The considered anemometer observations, as most other observations considered in this study, have been collected by the Dutch Government

(see `http://matroos.rws.nl/`). LiDAR wind velocity observations at vertical levels 63 m, 91 m, 116 m, 141 m, 166 m, 191 m and 241 m at K13 from the Dutch organization for applied research (TNO) have also been made available and are also considered in the validation of the wind data, in particular the variations with height. The validation against the fixed stations observations is complemented using winds at 10 m height from the Dutch Meteorological Institute (KNMI) operational Numerical Weather Prediction model Hirlam7.2 (KNMI, 2009) to evaluate the wind velocity spatial variations during the reporting period.

- The wave heights, periods and directions are also validated against Dutch Government observations. The locations for validating the buoy wave data are F3 and Schiermonnikoog Noord, referred to as SON and at about 62 km from the TNW buoys.
- The Dutch Government observations at K13 and SON are used for validating the water temperature.
- Available online data (`https://mesonet.agron.iastate.edu/request/download.phtml?network=NL__ASOS`) from weather stations located at Buitengaats, referred to as BG and located within the TNW region, are used for validating the air temperature.
- Dutch Government observations at K13, F3 and L91 are used for validating air pressure.
- Lastly, given the lack of fixed observation sources, the currents and water levels are validated against predictions from a purposely run by Deltares 3D hydrodynamic model.

Figure 1.2 shows an overview of all measurement locations. The present report provides the validation results for the period - 'January 2021' - extending from January 01 00:00 to January 31 23:50.

Figure 1.2: *Aerial view of the location of the buoys and fixed measurement stations (via Google Earth).*

All comparisons are presented as a timeseries and further validated via direct scatter plots for quantifying statistical correspondence between the datasets.

The error statistics are computed differently whether a linear or circular (directional) variable

is considered. For linear variables we have:

- the bias: $\bar{y} - \bar{x}$;
- the root-mean-square error: rmse = $\sqrt{n^{-1} \sum (y_i - x_i)^2}$;
- the symmetric slope: s = $\sqrt{\sum y_i^2 / \sum x_i^2}$; and
- the correlation coefficient:

$$r = \sum \left[(x_i - \bar{x})(y_i - \bar{y}) \right] / \sqrt{\sum (x_i - \bar{x})^2 \sum (y_i - \bar{y})^2} \;.$$

In all these formulae x_i usually represents observations (or the dataset which is considered less uncertain or baseline) and in this study we use it to represent the fixed observations, y_i usually represents the model results (or the dataset which is considered more uncertain or with a certain deviation from the baseline results) and in this study we use it to represent the TNWA and TNWB data and n the number of observations.

When dealing with circular data, each observation is considered as unit vector, and it requires vector addition rather than ordinary (or scalar) addition to compute the average of angles, the so-called mean direction.

Writing

$$C_n = \sum_{i=1}^{n} \cos x_i \quad and \quad S_n = \sum_{i=1}^{n} \sin x_i, \tag{1.1}$$

the sample resultant vector R_n of a sample $\mathbf{x} = x_i, \; i = 1, ..., n$ is defined as $R_n = \sqrt{C_n^2 + S_n^2}$, and its sample mean direction $\bar{x} \equiv \bar{x}_n$ as the direction of R_n:

$$\bar{x} = TAN^{-1}(S_n / C_n)$$

where

$$TAN^{-1}(S_n / C_n)$$

is the inverse of the tangent of

$$(S_n / C_n)$$

in the range [0, 2π], i.e.,

$$TAN^{-1}(S_n / C_n) := \begin{cases} \tan^{-1}(S_n / C_n), & S_n > 0, \; C_n > 0 \\ \tan^{-1}(S_n / C_n) + \pi, & C_n < 0 \\ \tan^{-1}(S_n / C_n) + 2\pi, & S_n < 0, \; C_n > 0. \end{cases} \tag{1.2}$$

The sample mean resultant length of $\mathbf{x} = x_i, \; i = 1, ..., n$ is defined by $\bar{R}_n = R_n / n$, $0 \le \bar{R}_n \le 1$. If $\bar{R}_n = 1$, then all angles coincide.

Equation 1.2 can be used to compute the bias between two circular variables by substituting x_i by $y_i - x_i$ in Equation 1.1. In a similar way, the root-mean-square error between two circular variables can be computed.

There are several circular analogues of the correlation coefficient, but the most widely used is the so-called T-linear correlation coefficient (Fisher and Lee (1983) and Fisher (1993)). Given

two sets $\mathbf{x} = x_i,\ i = 1,...,n$, $\mathbf{y} = y_i,\ i = 1,...,n$ of circular data, the T-linear correlation coefficient between x and y is defined by

$$r = \frac{\sum\limits_{1 \le i < j \le n} \sin(x_i - x_j) \sin(y_i - y_j)}{\sqrt{\sum\limits_{1 \le i < j \le n} \sin^2(x_i - x_j) \sum\limits_{1 \le i < j \le n} \sin^2(y_i - y_j)}}. \tag{1.3}$$

In the following we shall refer to comparisons in which r is higher than 0.9 as excellent, between 0.8 and 0.9 as good, between 0.7 and 0.8 as reasonable and lower than 0.7 as poor. Note that this is no absolute quality statement given that there are uncertainties in both observations and, due to the distance between the instruments, the spatial variability is expected to affect the comparisons.

Note that all reported dates are in GMT (which is equivalent to UTC).

1.1 Outline of the report

The availability of the considered TNW data is given in the next chapter, followed by the description and validation of the wind, wave, temperature, pressure, water level and current data in separate chapters. A summary of the drawn conclusions is given in the executive summary at the start of this report.

2 Data Availability

Although in measuring campaigns the aim is always of having a full (gap free) timeseries of all measured parameters, they are typically hampered by severe metocean conditions and loss of signal between instruments. Figure 2.1 shows a detailed breakdown for each buoy of the amount of missing data throughout the temporal record for each measured parameter. The availability of the data is computed from January 01 00:00 to January 31 23:50. Note that in this validation study only processed data (10 minute averages in the case of wind) are considered. The original raw observations have been processed and quality checked by Fugro. Furthermore, data from all processed variables are supposed to be available every 10 minutes (at the hour and 10, 20 30, 40 and 50 minutes after the hour). Table 2.1 gives a brief explanation of what the variable names in Figure 2.1 mean, their units and, if applicable, the symbols used to refer to them.

As can be seen in Figure 2.1, the collected data consists of wind speed and direction at different heights, a number of wave height, period and direction parameters, current speed and direction at different depths, water and air temperature, pressure and humidity.

We use the following qualification of data availability:

- >95% referred to as high availability,
- 90 - 95% referred to as good availability,
- 80 - 90% referred to as acceptable availability,
- 60 - 80% referred to as limited availability, and
- <60% referred to as poor availability.

Because the buoy has only been deployed on the 16th of January 2021, the availability of all data from TNWA-2 is poor. Unfortunately, the availability of current, water level and bottom temperature data from TNWB is also poor. On the other hand, the availability of wave, air pressure and air and surface water temperature data from TNWB is high. The availability of wind data from TNWB is also high, except for the LiDAR wind direction data which is acceptable, with most of the data missing after the 26th of January when data from TNWA-2 are available.

Not all data being measured are considered in this report:

- Although the availability of the humidity data is given in Figure 2.1, the data are not considered further.
- The buoys are also recording the wave spectra, but they are not transmitted on an ongoing basis and therefore also not considered on a monthly basis.
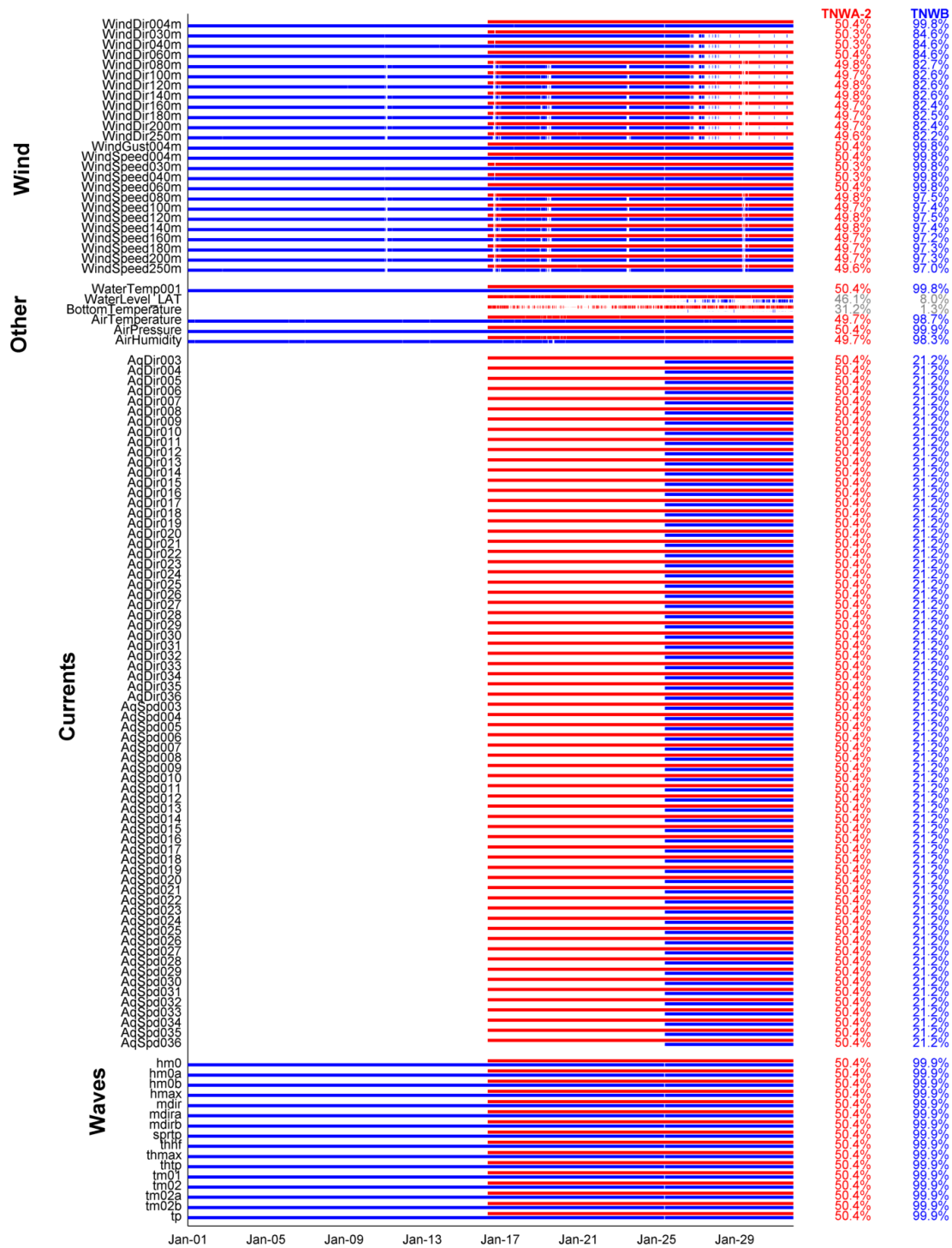
Figure 2.1: *Availability of the 10 minute TNWA-2 (red), TNWB (blue) and WLS (grey) data of January 2021.*

Table 2.1: *List of variables.*

Name	Description	Units	Symbol
WindSpeed z mh	Wind speed at an elevation of z m above the sea surface	m/s	U_z
WindGust z mh	Wind gust speed at an elevation of z m above the sea surface	m/s	
WindDir z m	Wind direction at an elevation of z m above the sea surface	°N	$U_{z\theta}$
airTemperature	Air temperature	°C	T_{air}
airPressure	Air pressure	hPa	
airHumidity	Air humidity	%	
WaterTemp001	Water temperature (surface)	°C	T_{water}
WaterLevel	Still water level	m LAT	WL
BottomTemp	Water temperature (bottom)	°C	T_{water}
AqSpd d	Current speed at a depth of d m below the sea surface	m/s	u_d
AqDir d	Current direction at a depth of d m below the sea surface	°N	
hm0	Spectral significant wave height	m	H_s
hm0a	Spectral significant swell wave height. Frequency band between 0.04 and 0.10 Hz.	m	H_{sswell}
hm0b	Spectral significant sea wave height. Frequency band between 0.10 and 0.50 Hz.	m	H_{ssea}
hmax	Spectral maximal individual wave height	m	H_{max}
mdir	Mean wave direction	°N	MWD
mdira	Mean wave direction of swell	°N	MWD_{swell}
mdirb	Mean wave direction of sea	°N	MWD_{sea}
sprtp	Wave spreading at spectral peak period	°	$DSPR$
thhf	High frequency mean wave direction. Frequency band between 0.4 and 0.44 Hz.	°N	
thmax	Period of highest wave.	s	$T_{H_{max}}$
thtp	Wave direction at spectral peak period.	°N	
tm0x	Spectral mean absolute wave period (1 based on the 1st spectral moment, 2 based on the 2nd spectral moment, a swell, b sea)	s	T_{m0x}
tp	Spectral peak wave period	s	T_p

3 Wind

This chapter focuses on the validation of the wind velocity observations from the *SEAWATCH LiDAR Buoys*. The wind speed and direction are measured at 4 m above water level by a Sonic wind sensor and at levels 30, 40, 60, 80, 100, 120, 140, 160, 180, 200 and 250 m above water level by a LiDAR.

An overview and intercomparison of the TNW wind data is given next, followed by a validation using observed and model data.

Given that for low wind speeds there is much scatter in the data and that these data are not relevant in the data analyses (profiles and error statistics), all observations for which the observed wind speeds are below 5 m/s are excluded. This threshold was chosen pragmatically, being in line with the work of Wieringa and Rijkoort (1983) and in line with other wind climate assessments of the Dutch meteorological institute and close to the 4 m/s threshold prescribed for the calibration of cup anemometers in the IEC 61400-12-1 standard.

3.1 Ten Noorden van de Waddeneilanden description and intercomparison

To get a full overview of the data two movies are created with the time evolution of vertical wind profiles at TNWA-2 (see here) and at TNWB (see here).

Figure 3.1 and Figure 3.2 show the timeseries of respectively the wind speed and direction at the observation levels. The figures show that both buoys have observed the first named storm of 2021, the southwestern storm Christoph on the 21st, during which the wind speeds peaked above 30 m/s with large gradients in height. During the rest of the month the wind speeds are generally below 20 m/s, except for on the 11th (13th) of January when the winds from Southwest (Northwest) and peaking above 20 m/s are observed at TNWB.
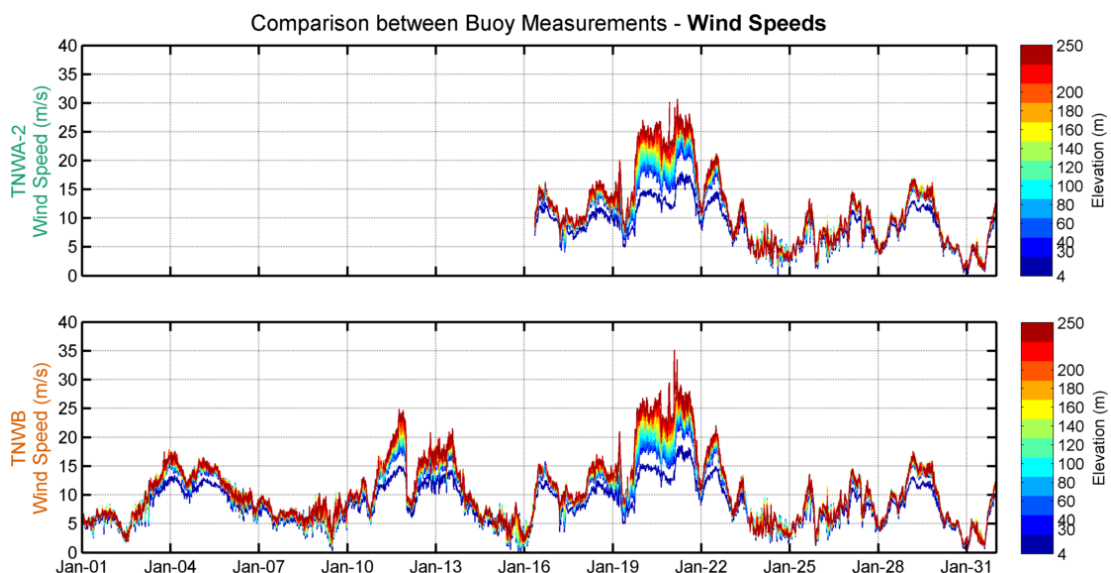
Figure 3.1: Wind speeds (by elevation) at each buoy.
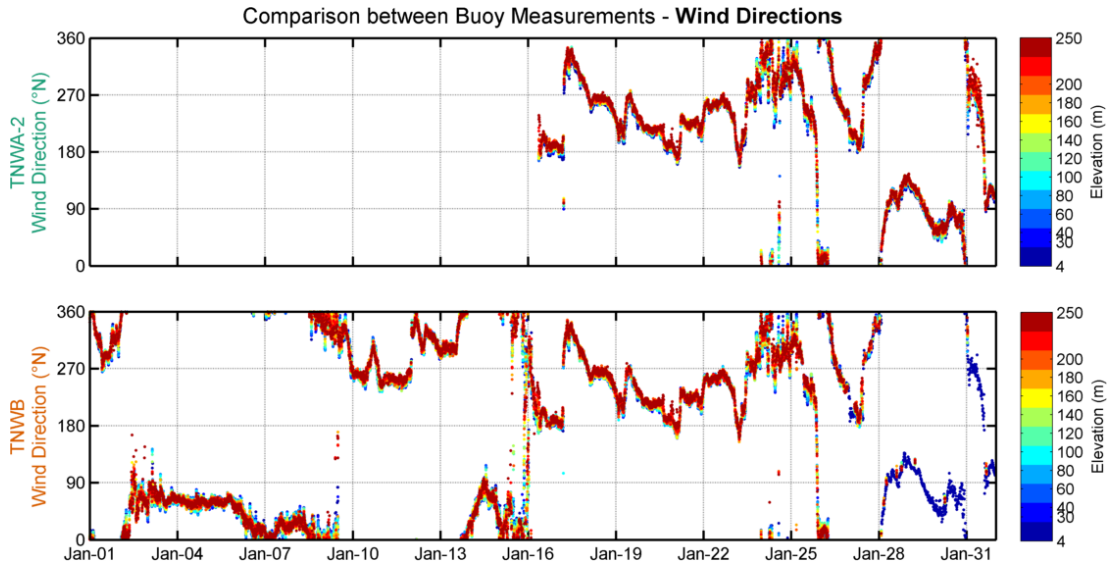
Figure 3.2: *Wind directions (by elevation) at each buoy.*

Figure 3.3 provides an overview of the observed LiDAR data without the filtered low observations. The figure shows all observed vertical profiles for which the wind speed is above 5 m/s (grey lines), the mean profile (red line) and a fitted power profile (blue line).

The power law profile is described by:

$$U(z) = U_{30}\left(\frac{z}{30}\right)^{\alpha}$$

where U_{30} is the wind speed at 30m above the surface and α is the power-law constant. The fit given in Figure 3.3 has been obtained using least squares.

Figure 3.3 shows that the mean power law profile matches almost perfectly the mean observed vertical wind profile, and the power-law constant of the TNWA-2 data is higher than that of the TNWB data, given that on average the wind speeds are higher in the period covered by the TNWA-2 data.
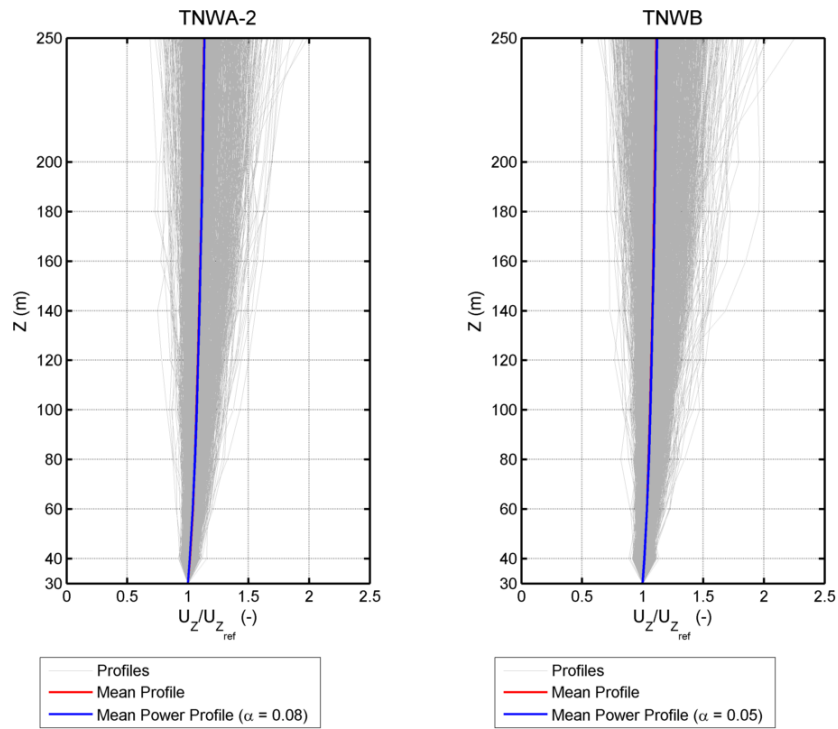
Figure 3.3: *Normalized LiDAR wind speed vertical profiles (data from January 2021).*

Figure 3.4 shows density scatter comparisons between the wind speed and direction measured by TNWA-2 and TNWB at two chosen levels, 100m and 160m. The figure shows a general agreement between the observation of TNWA-2 and TNWB, as could already be seen in figures 3.1 and 3.2.
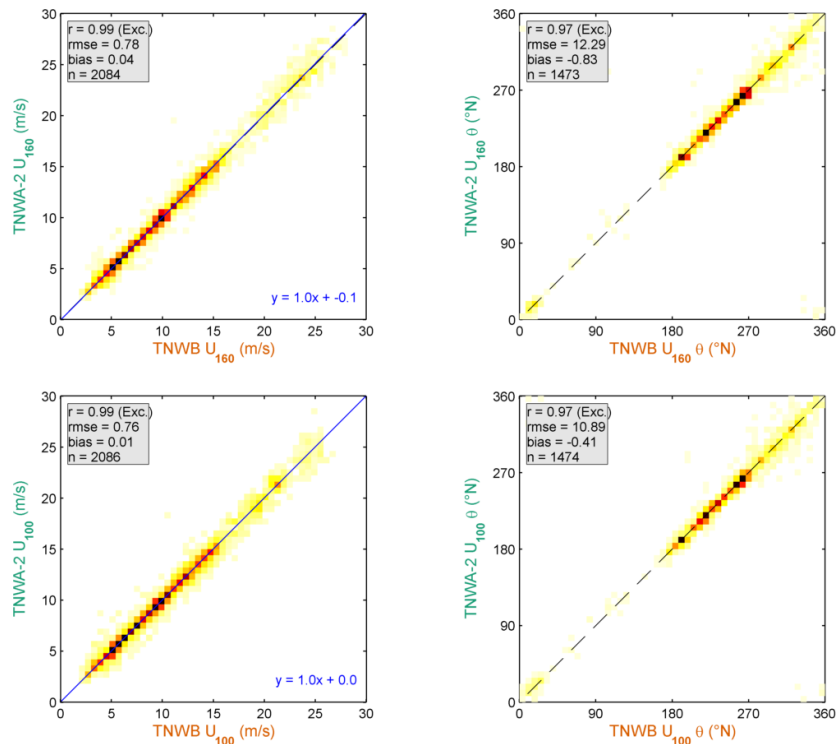
Figure 3.4: *Direct scatter comparison between LiDAR wind at 100 and 160 m (data from January 2021).*

In order to further quantify the differences between the TNWA-2 and TNWB wind speed and direction observations, the slope, bias, correlations and square correlations between the TNWA-2 and TNWB wind speed observations at all levels and the bias, correlations and square correlations between the TNWA-2 and TNWB wind direction observations at all levels have been computed considering all wind speeds above 2 m/s. These are given in Table 3.1 and (given the lower threshold) can be compared against the criteria given in IEC 61400-12-1 (2017) and IEA Wind (2017)[1]. The table shows that, even applying such a low wind speed threshold, the comparisons are at all levels excellent both in terms of wind speed and direction. Table 3.1 also shows that the correlations between the wind directions are lower than between the wind speeds and also that the sizes of the collocated wind direction samples is lower than of the collocated wind speed samples, due to the missing TNWB wind direction data.

Table 3.1: *Statistical comparison between the winds from the LiDAR buoys with elevation.*

Elev. (m)	Wind Speed					Wind Direction			
	r^2 (-)	r (-)	Bias (m/s)	Sym. Slope (-)	n (-)	r^2 (-)	r (-)	Bias (°)	n (-)
4	0.96	0.98	0.08	1.01	2159	0.94	0.97	1.9	2159
30	0.97	0.99	-0.02	1.00	2179	0.93	0.97	-0.4	1544
40	0.97	0.99	-0.03	1.00	2179	0.93	0.96	-0.5	1546
60	0.98	0.99	-0.02	1.00	2192	0.94	0.97	-0.6	1556
80	0.98	0.99	0.00	1.00	2088	0.94	0.97	-0.7	1476
100	0.98	0.99	0.01	1.00	2086	0.94	0.97	-0.4	1474
120	0.98	0.99	0.02	1.00	2081	0.94	0.97	-0.6	1471
140	0.98	0.99	0.04	1.00	2086	0.94	0.97	-0.6	1476
160	0.98	0.99	0.04	1.00	2084	0.93	0.97	-0.8	1473
180	0.98	0.99	0.04	1.01	2085	0.93	0.96	-0.3	1475
200	0.98	0.99	0.05	1.01	2086	0.93	0.96	-0.3	1476
250	0.98	0.99	0.03	1.01	2070	0.92	0.96	-0.3	1467

3.2 Validation

In this section the TNWA-2 (Section 3.2.2) and TNWB (Section 3.2.3) wind data at a single level are validated against anemometer observations at L91 (at a height of z=87 m and at a distance of about d= 59 km from TNW), K13 (z=73.8 m, d=178 km), AWG (z=60 m, d=64 km), and HG (z=18 m, d=75 km). The wind speeds at several levels are validated against LiDAR observations at K13 (z=63, 91, 116, 141, 166, 191 and 241 m). Note that K13 is at a considerable distance from TNWA-2 and TNWB and in periods with large spatial wind variations comparisons between these data can be expected to be poor. Furthermore, given its proximity to the coast, the winds blowing from the coast at HG and AWG are expected to be more strongly influenced by land effects. Nevertheless, data from these stations are still expected to show some correspondence with the TNW data and in any case to provide a measure of spatial variability and also variability in height.

An overview of the comparisons between the TNW and the fixed platform anemometer datasets is presented first, followed by a comparison of each TNWA-2 and TNWB datasets with measured fixed platform anemometer and LiDAR data. Finally, the spatial variability of the wind is evaluated using model data.

---

[1]Note that the applied T-linear correlation coefficient Equation 1.3 leads in general to slightly lower correlations between directions than those using the standard correlation as in the cited criteria.

3.2.1 Overview

Figure 3.5 provides an overview of the comparisons, comparing the timeseries of the L91, K13, AWG, and HG observations and the TNWA-2 and TNWB LiDAR observations at the levels closer to those the anemometers. A further overview of the comparisons between data at the buoy and platform locations is given by means of wind roses at Figure 3.6. Given the lack of wind direction data, Figure 3.6 contains no rose of the K13 data. Note that the periods covered by the data differ per dataset, nevertheless there is a general alignment between the datasets, with the southwestern winds from storm Christoph being the stronger that have been observed at all locations.
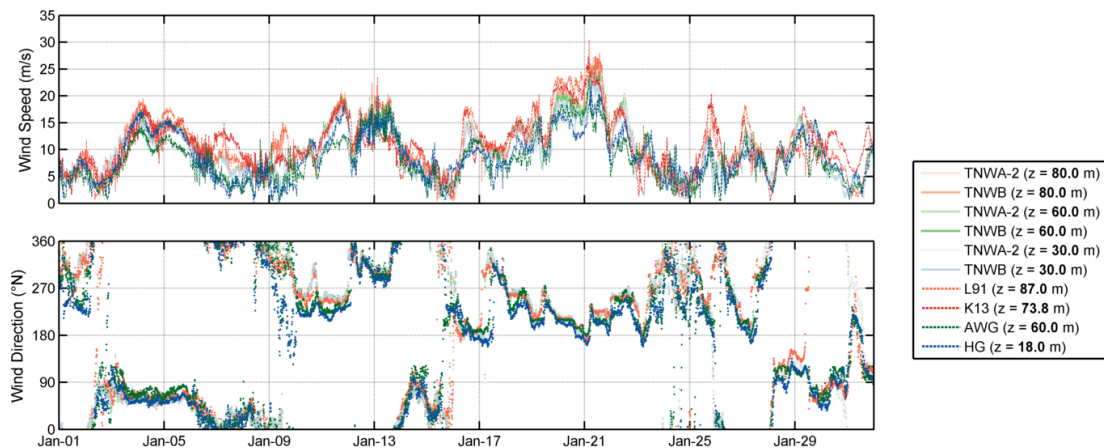
Figure 3.5: *Wind speed and direction for all locations (data from January 2021).*
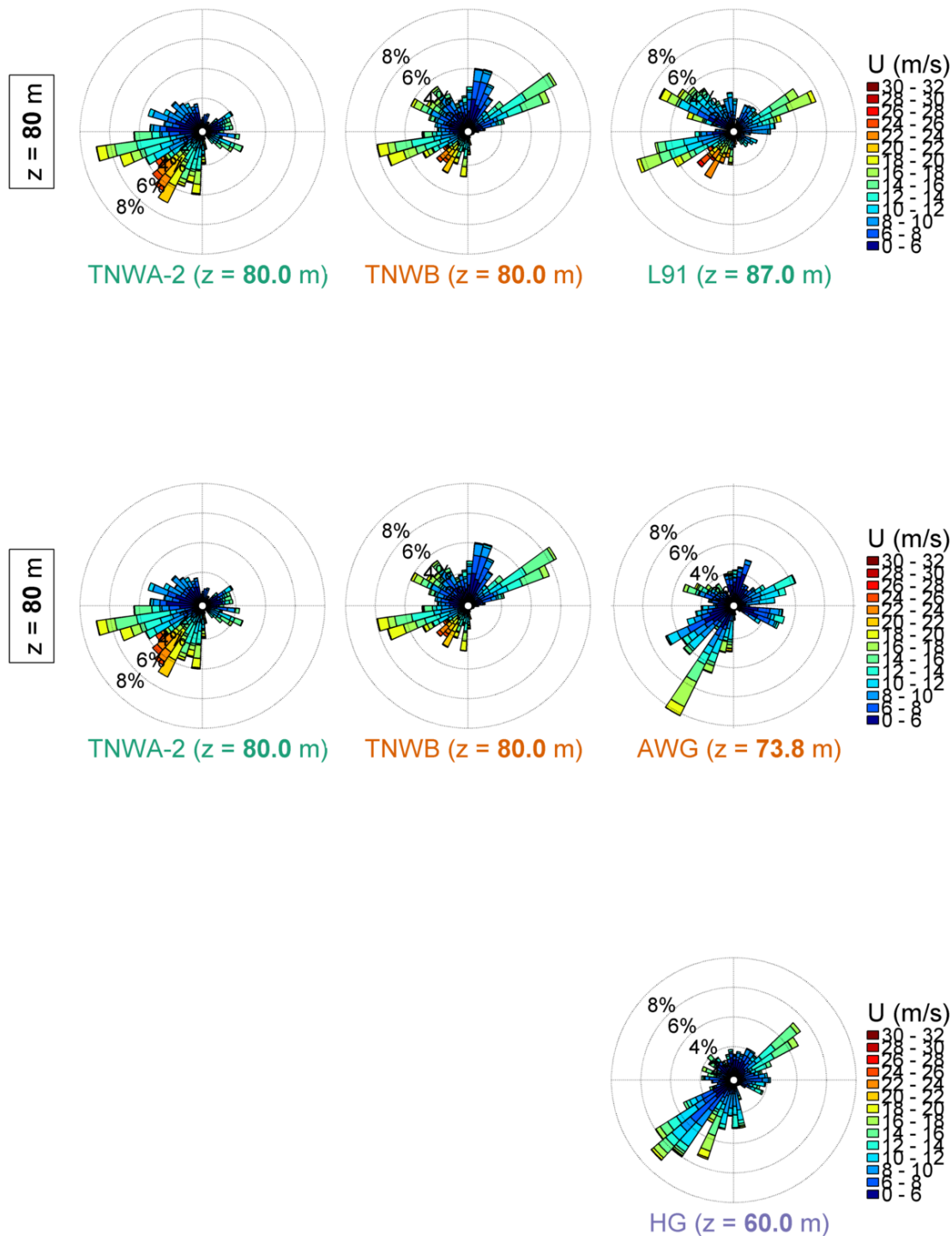
Figure 3.6: *Wind roses (of bin width 8°) for all locations (data from January 2021).*

3.2.2 Ten Noorden van de Waddeneilanden Buoy TNWA-2

3.2.2.1 Anemometer

Figures 3.7, 3.8, 3.9 and 3.10 show comparisons between TNWA-2 observations and those at L91, K13, AWG, and HG, respectively. The correlation, root-mean-square error and bias statistics are printed in the figures. As can be seen in the figures, the comparisons between the TNWA-2 observations and those from:

- L91 are good in terms of both wind speed and direction,
- K13 are reasonable in terms of wind speed (there are no wind direction data available from K13),
- AWG are reasonable terms of wind speed and good in terms of wind direction, and
- HG are good in terms of wind speed and reasonable in terms of wind direction.

The lower correlations in terms of wind directions at HG are to a large extent due to the mismatches in the period of varying wind directions between the 24th and the 25th. The lower correlations in terms of wind speeds at K13 and AWG are to a large extent due to the mismatches in the periods of eastern winds, when spatial variations can be expected.

Figure 3.7: *Validation of TNWA-2 (data from January 2021) with L91 wind data. Top panels: Wind speed timeseries (left) and density scatter (darker colours indicating higher data density) and linear fit line (right). Bottom panels: Wind direction timeseries (left) and density scatter (right).*
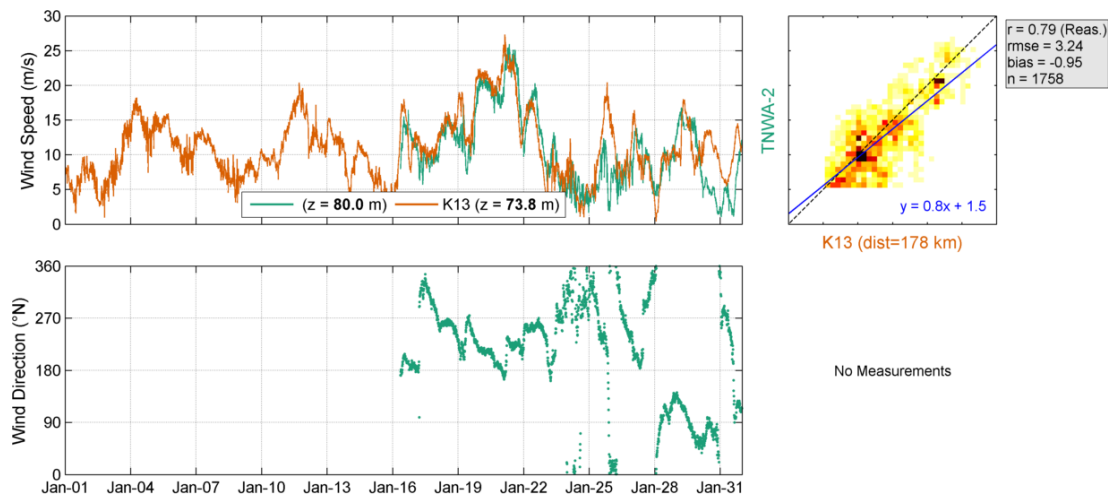
Figure 3.8: *Validation of TNWA-2 (data from January 2021) with K13 wind data. Top panels: Wind speed timeseries (left) and density scatter (darker colours indicating higher data density) and linear fit line (right). Bottom panels: Wind direction timeseries (left) and density scatter (right).*
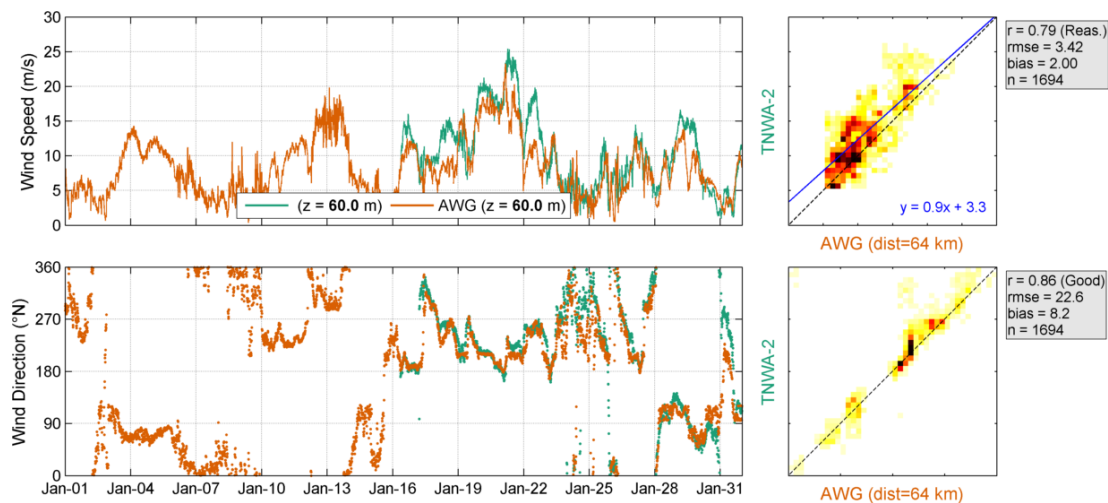
Figure 3.9: *Validation of TNWA-2 (data from January 2021) with AWG wind data. Top panels: Wind speed timeseries (left) and density scatter (darker colours indicating higher data density) and linear fit line (right). Bottom panels: Wind direction timeseries (left) and density scatter (right).*
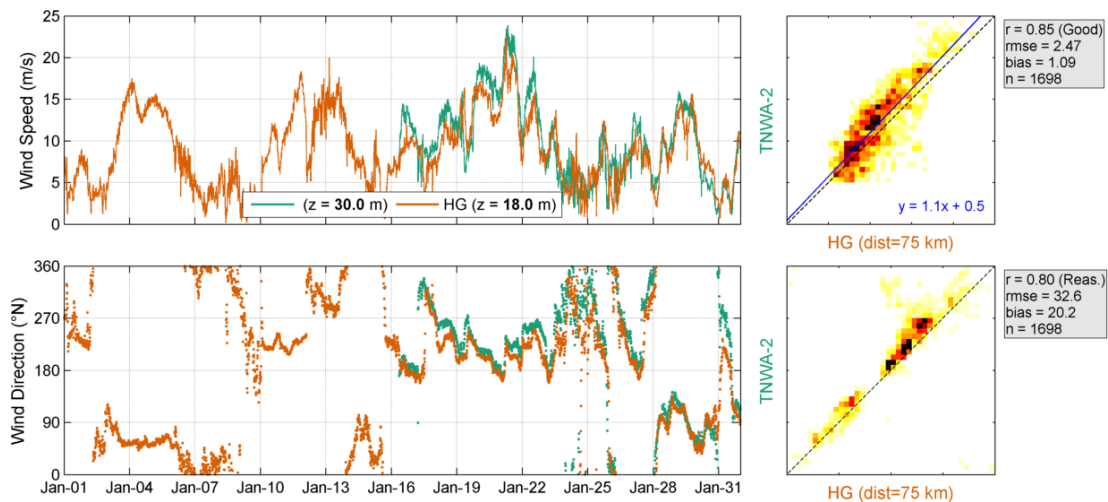
Figure 3.10: *Validation of TNWA-2 (data from January 2021) with HG wind data. Top panels: Wind speed timeseries (left) and density scatter (darker colours indicating higher data density) and linear fit line (right). Bottom panels: Wind direction timeseries (left) and density scatter (right).*

3.2.2.2 LiDAR

In the following the TNWA-2 wind data are compared with the LiDAR observations at K13. Before comparing the TNWA-2 data with the K13 LiDAR data, these are validated against the anemometer data at K13. Figure 3.11 shows the comparison between the K13 LiDAR and anemometer timeseries. A timeseries comparison is provided (by elevation), with a density scatter comparing the best match (in terms of elevation) between the two datasets. I.e., the LiDAR measurements at the 63 m level are directly compared against the anemometer observations at the 73.8 m level. The correlation between the wind speeds is excellent, with the (observed at a higher height) anemometer wind speeds being as expected on average higher.

Table 3.2 shows the comparisons between the TNWA-2 observations and those of the closer vertical levels by the LiDAR at K13. The comparisons are reasonable (lower level) to good (all other levels) in terms of wind speed and poor in terms of wind direction. The lower wind speed correlations at the lower level indicate larger spatial variability of the lower wind speeds. The poor correlations in terms of wind direction are also expected to be due to spatial variations, in particular in the periods of low eastern winds.
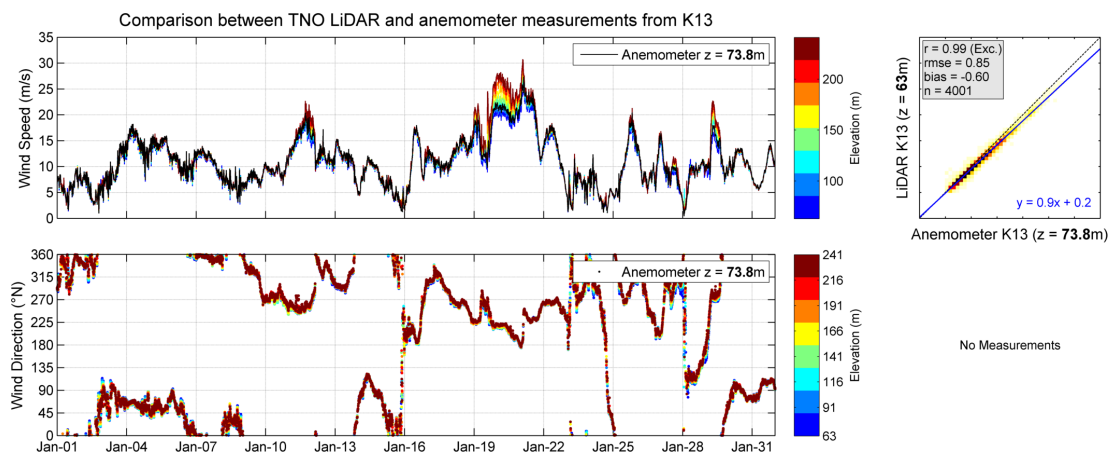
Figure 3.11: *Comparison between ECN LiDAR and anemometer measurements at K13.*

Table 3.2: *Statistical comparison between TNWA-2 and K13 LiDARs at different heights.*

Elevation		Wind Speed				Wind Direction		
TNWA-2 (m)	K13 (m)	r (-)	Bias (m/s)	Symmetrical Slope (-)	n (-)	r (-)	Bias ($^\circ$)	n (-)
60	63	0.77	0.40	1.02	1784	0.50	12.5	1784
100	91	0.80	0.40	1.02	1759	0.53	10.8	1759
120	116	0.81	0.52	1.03	1756	0.52	11.3	1756
140	141	0.82	0.62	1.03	1762	0.53	10.9	1762
160	166	0.82	0.71	1.04	1759	0.54	11.1	1759
200	191	0.83	0.71	1.04	1763	0.54	11.1	1763
250	241	0.83	0.74	1.04	1765	0.54	10.6	1765

3.2.3 Ten Noorden van de Waddeneilanden Buoy TNWB

3.2.3.1 Anemometer

As shown for TNWA-2, figures 3.12, 3.13, 3.14 and 3.15 show comparisons between TNWB observations and those at L91, K13, AWG, and HG, respectively. The correlation, root-mean-square error and bias statistics are printed in the figures. As can be seen in the figures, the comparisons between the TNWA-2 observations and those from:

- L91 are good in terms of both wind speed and direction,
- K13 are reasonable in terms of wind speed,
- AWG are reasonable in terms of both wind speed and direction, and
- HG are good in terms of wind speed and reasonable in terms of wind direction.

As in the comparisons between the TNWA-2 and the fixed stations data, the mismatches between the TNWB and the fixed stations data can be explained by spatial variabilities in particular in periods of low wind speeds.
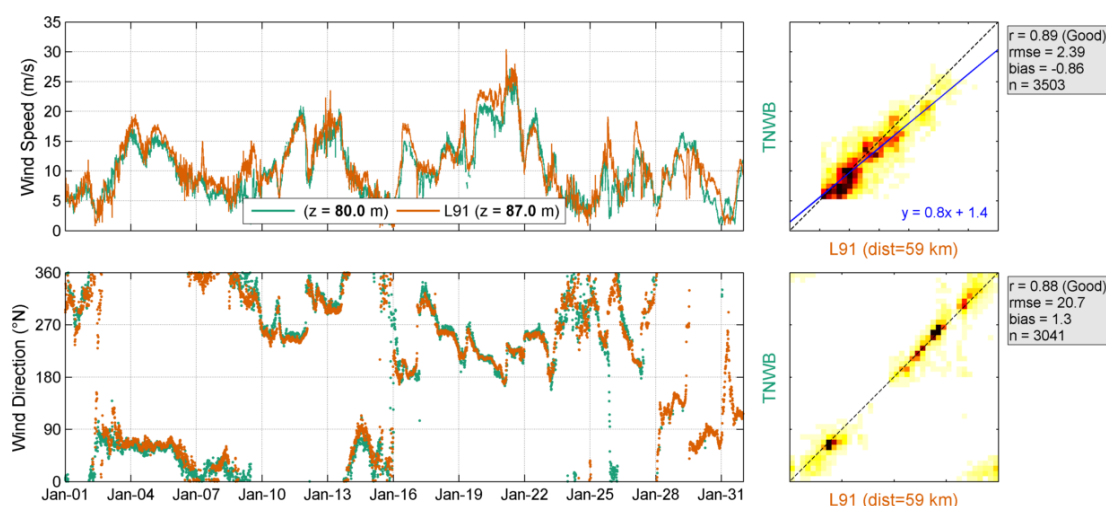
Figure 3.12: *Validation of TNWB (data from January 2021) with L91 wind data. Top panels: Wind speed timeseries (left) and density scatter (darker colours indicating higher data density) and linear fit line (right). Bottom panels: Wind direction timeseries (left) and density scatter (right).*
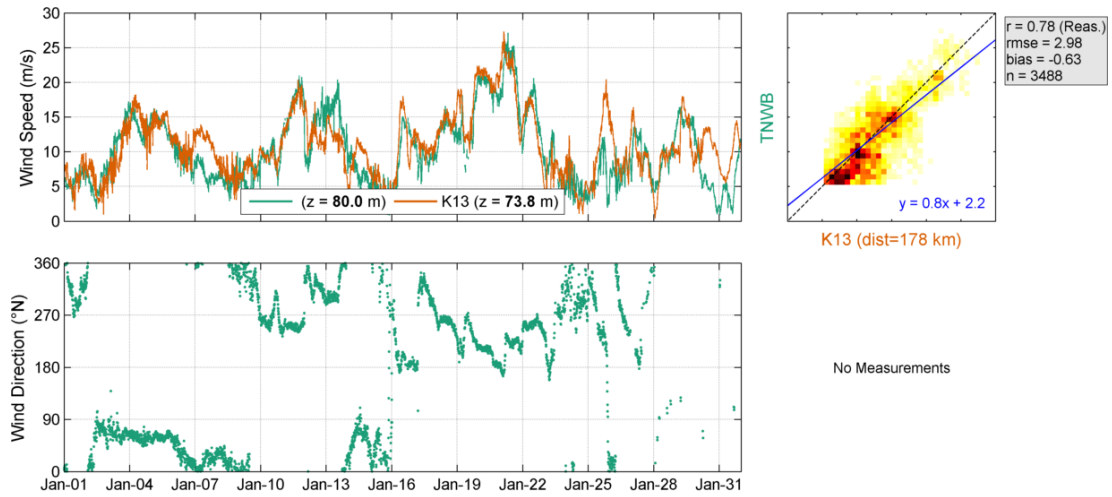
Figure 3.13: *Validation of TNWB (data from January 2021) with K13 wind data. Top panels: Wind speed timeseries (left) and density scatter (darker colours indicating higher data density) and linear fit line (right). Bottom panels: Wind direction timeseries (left) and density scatter (right).*
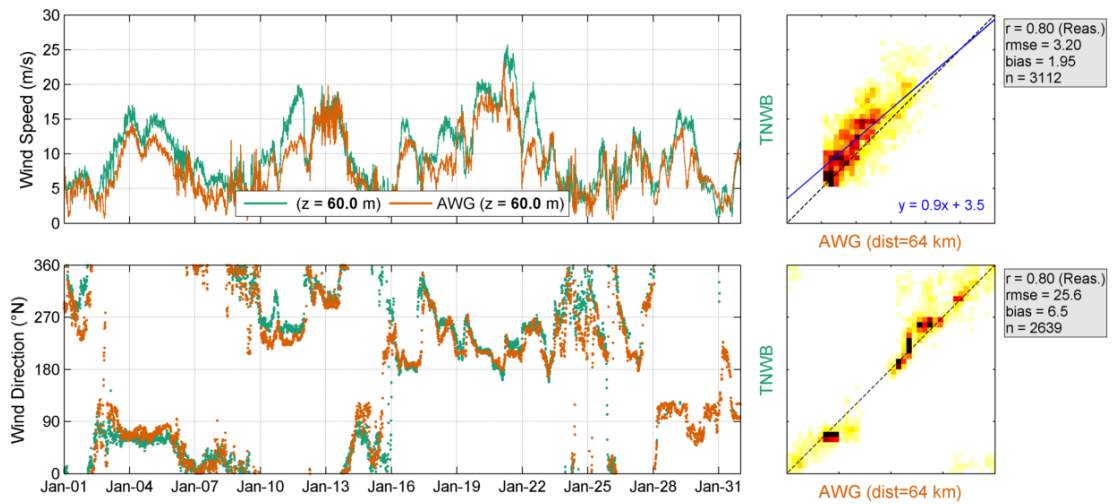
Figure 3.14: *Validation of TNWB (data from January 2021) with AWG wind data. Top panels: Wind speed timeseries (left) and density scatter (darker colours indicating higher data density) and linear fit line (right). Bottom panels: Wind direction timeseries (left) and density scatter (right).*
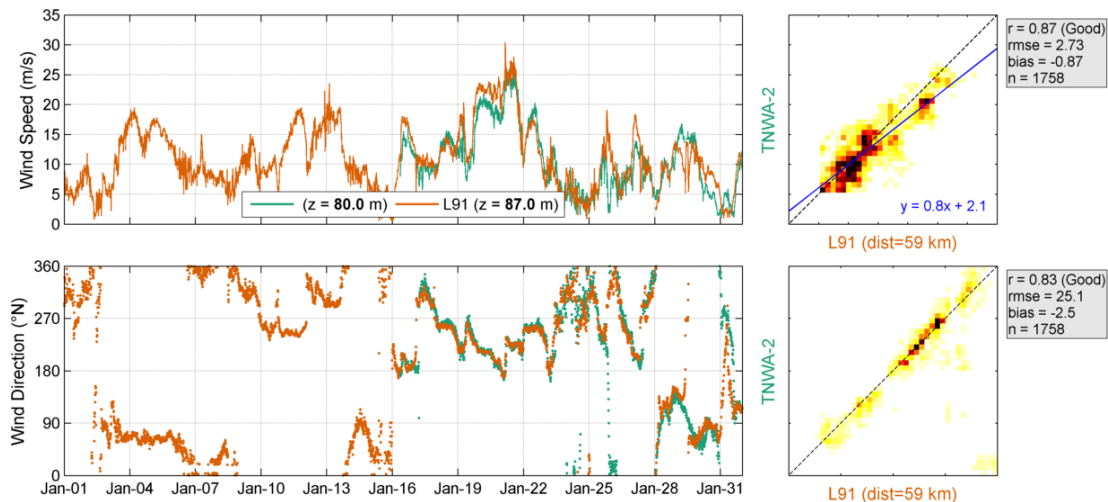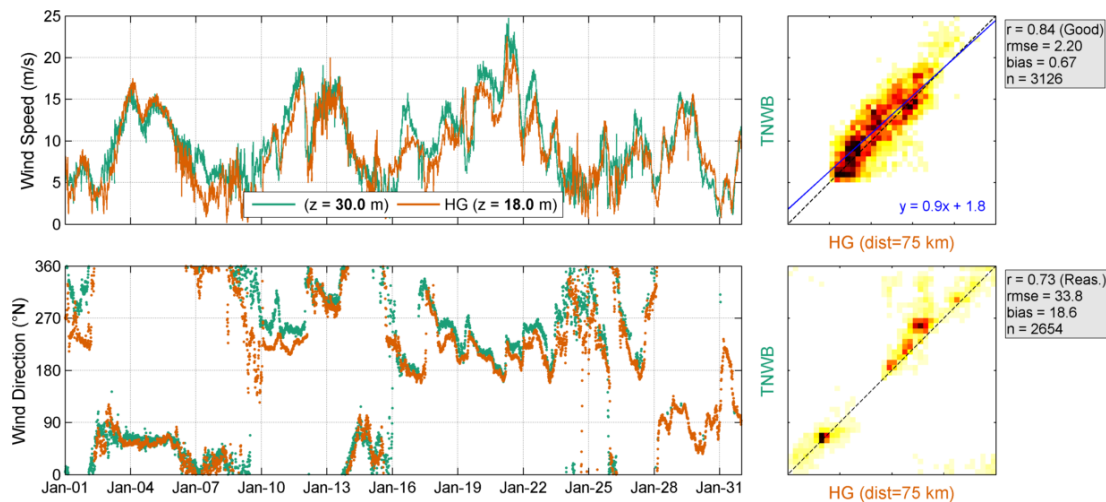
Figure 3.15: *Validation of TNWB (data from January 2021) with HG wind data. Top panels: Wind speed timeseries (left) and density scatter (darker colours indicating higher data density) and linear fit line (right). Bottom panels: Wind direction timeseries (left) and density scatter (right).*

3.2.3.2 LiDAR

Table 3.3 show the error statistics between the TNWB observations and those of the closer vertical levels by the LiDARs at K13. The comparisons are reasonable to good in terms of wind speed and at all levels reasonable in terms of wind direction. The increase of the correlation between wind speeds with height indicate again that the mismatches occur mainly due to spatial variations when the wind speeds are lower.

Table 3.3: *Statistical comparison between TNWB and K13 LiDARs at different heights.*

Elevation		Wind Speed				Wind Direction		
TNWB (m)	K13 (m)	r (-)	Bias (m/s)	Symmetrical Slope (-)	n (-)	r (-)	Bias (°)	n (-)
60	63	0.76	0.19	1.00	3565	0.73	5.2	3074
100	91	0.79	0.14	0.99	3496	0.75	4.8	3020
120	116	0.80	0.19	1.00	3514	0.76	4.6	3036
140	141	0.80	0.24	1.00	3526	0.77	4.5	3046
160	166	0.81	0.27	1.01	3528	0.77	4.8	3052
200	191	0.82	0.24	1.00	3554	0.78	4.7	3073
250	241	0.82	0.25	1.00	3554	0.78	4.7	3076

3.2.4 Spatial and temporal variability

In order to further evaluate the spatial variations in the observation period, the wind fields from the Dutch Meteorological Institute (KNMI) operational Numerical Weather Prediction model Hirlam7.2 are also considered. The model fields are only available at 10 m and with an hourly resolution. The spatial resolution of the model is about 11 km x 11 km, which implies that the model in principle underestimates the spatial variations and coastal effects, i.e. the model results can be expected to be smoother than the true fields.

In order to characterize further the most extreme event in the observation period, Figure 3.16 shows the model wind fields at the hour of the maximum observed 100 m wind speed at TNW, which was observed at 8:00 at TNWA-2 and 7:40 at TNWB on the 21th of January (cf. Figure 3.1). The figure shows storm Christoph winds from the Southwest with the higher model wind speeds north of the TNW buoy locations.
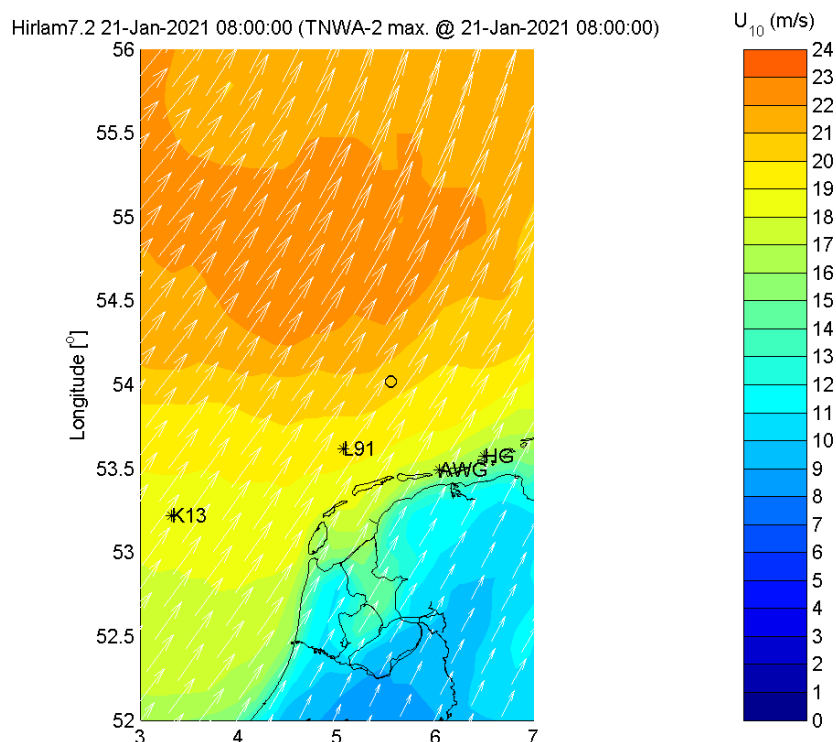
Figure 3.16: *Hirlam7.2 surface (10 m) wind field at the hour of the maximum TNWA-2 and TNWB 100 m wind speed. The *s indicate the locations of the fixed stations and the ∘s the TNW locations.*

Table 3.4 shows the correlations between the Hirlam7.2 10 m (hourly) wind speeds and directions from the model grid points closer to the buoy and the fixed station locations at the timestamps at which the data from each of the buoys are valid. Given the proximity of the TNWA-2 and TNWB locations the considered model grid point is the same, therefore differences between correlations with the data at the TNWA-2 and TNWB locations are only due to differences in measurement data availability. For these periods the corresponding correlations between the buoy and the fixed station anemometer (10 minute) observations (at the closer vertical levels) are given in figures 3.7 to 3.10 and 3.12 to 3.15 and reproduced Table 3.5. As can be seen in Table 3.4, the model winds at TNW have the higher correlations with the winds at the L91 and the lowest with the winds at K13. The comparison of the correlations between the observations and the models results confirm that the found

discrepancies are mostly due to spatial variations (note also the low correlations between the TNW and K13) and local effects (such as land effects at AWG and HG) which are less present in the model results due to its resolution.

Table 3.4: *Statistical comparison between the model results at the buoy and at the fixed station locations at the timestamps at which the buoy data are valid*

Station	TNWA-2			TNWB		
	U_{10} r **(-)**	U_{dir} r **(-)**	n **(-)**	U_{10} r **(-)**	U_{dir} r **(-)**	n **(-)**
L91	0.91	0.91	309	0.91	0.94	622
K13	0.80	0.51	309	0.78	0.67	622
AWG	0.92	0.90	309	0.92	0.93	622
HG	0.90	0.81	309	0.89	0.81	622

Table 3.5: *Statistical comparison between the TNWA-2 and TNWB buoy observations and those from the fixed stations.*

Station	TNWA-2				TNWB			
	U_h r **(-)**	n **(-)**	U_{dir} r **(-)**	n **(-)**	U_h r **(-)**	n **(-)**	U_{dir} r **(-)**	n **(-)**
L91	0.87	1758	0.83	1758	0.89	3503	0.88	3041
K13	0.79	1758	-	-	0.78	3488	-	-
K13 (LiDAR)	0.77-0.83	1756	0.50-0.54	1756	0.76-0.82	3496	0.73-0.78	3020
AWG	0.79	1694	0.86	1694	0.80	3112	0.80	2639
HG	0.85	1698	0.80	1698	0.84	3126	0.73	2654

3.3 Conclusions

Based on the comparisons between the data from the buoys, which are excellent at all levels, the validation of the data against observations and model data, which shows mismatches can be explained by local effects and spatial and vertical variations, it can be concluded that the accuracy of the TNW buoy wind speeds and directions is high.

4 Waves

The measured waves from both buoys are presented and analyzed within this chapter. The goal is to assess the reliability and accuracy of the retrieved wave data from both TNWA-2 and TNWB. This is completed by first comparing the integral parameters from both buoys against each other, followed by a statistical validation against fixed wave measurements in the area.

4.1 Overview

The timeseries of the main wave parameters from both TNWA-2 and TNWB are shown in Figure 4.1. Recall that the data from TNWB cover the whole period and the data from TNWA-2 are available from the 16th. The wave parameters plotted in Figure 4.1 are:

- significant wave height, H_s
- peak wave period, T_p
- mean wave direction, MWD
- swell and sea[1] significant wave heights, H_{sswell} and H_{ssea}
- maximum wave height, H_{max}
- swell and sea mean wave directions, MWD_{swell} and MWD_{sea}
- mean wave periods, T_{m01} and T_{m02}, and
- swell and sea mean wave periods, $T_{m02swell}$ and T_{m02sea}.

As can be seen in Figure 4.1, the most predominant waves are from the Northwest and the highest waves are from the Southwest during storm Christoph on the 21st. Furthermore, the observations from the two buoys at Ten Noorden van de Waddeneilanden agree extremely well given the near-identical signals (e.g. H_s, T_{m02}, etc ...) with only short term discrepancies between T_p, $T_{m02swell}$ and the mean wave direction of swell. These are expected given the generally low conditions and that these parameters depend more strongly on the sampling variability (randomness of the sea surface elevation) and discreteness of the wave spectra.

---

[1]The swell and sea variables are computed from the spectral energy in the frequency band between respectively 0.04 and 0.10 Hz and 0.10 and 0.50 Hz (cf. Table 2.1).
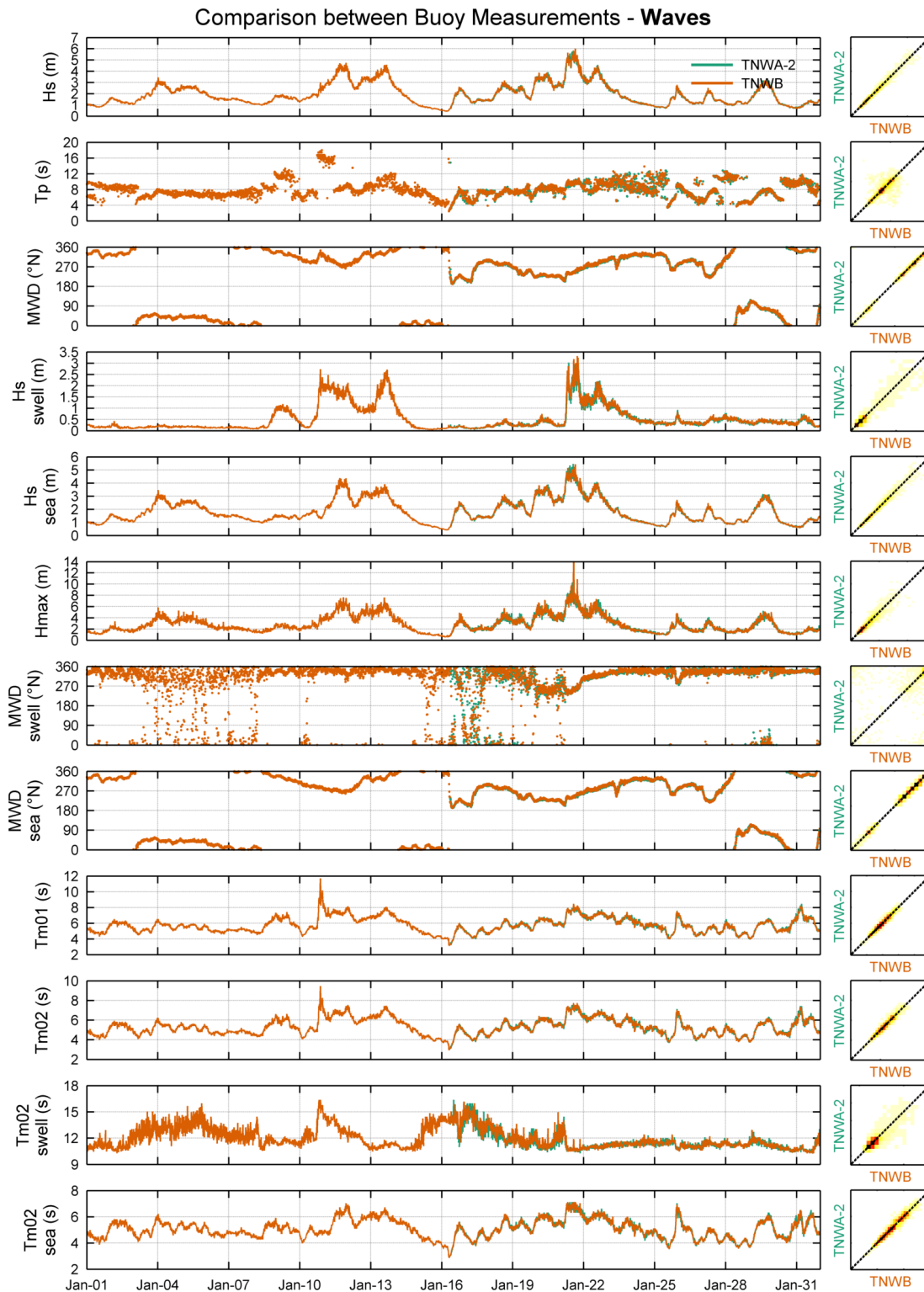
***Figure 4.1:** Wave parameters at each buoy (data from January 2021).*

The slope, bias, correlations and square correlations were calculated for all wave parameters measured at TNWA-2 and TNWB to quantify their statistical differences, see Table 4.1. As can be seen in the table, the agreement between the two buoys is excellent in terms of all parameters, except in terms of swell mean wave period which is good, peak wave period which is reasonable and mean wave direction which is poor. The mismatches in the mean

wave direction of swell are in periods with almost no swell energy (cf. Figure 4.1). These low levels of energy explain the variability in the resulting swell direction but also make it less important.

Table 4.1: *Statistical comparison between TNWA-2 and TNWB wave parameters.*

Parameter	Unit	r^2 (-)	r (-)	Bias (unit)	Symmetrical Slope (-)	n (-)
hm0	m	0.98	0.99	0.01	1.00	2246
tp	s	0.53	0.73	0.06	1.01	2246
mdir	°N	0.98	0.99	1.40	1.00	2246
hm0a	m	0.92	0.96	0.01	1.02	2246
hm0b	m	0.98	0.99	0.00	1.00	2246
hmax	m	0.89	0.94	0.04	1.02	2246
mdira	°N	0.42	0.65	1.69	1.00	2246
mdirb	°N	0.98	0.99	1.41	1.00	2246
tm01	s	0.95	0.97	0.01	1.00	2246
tm02	s	0.95	0.97	0.00	1.00	2246
tm02a	s	0.78	0.89	0.08	1.01	2246
tm02b	s	0.95	0.97	-0.00	1.00	2246

4.2 Validation

An overview of the comparisons is first presented, followed by a detailed comparison between the data from TNWA-2 (Section 4.2.2) and TNWB (Section 4.2.3) with the fixed observations.

4.2.1 Overview

Figure 4.2 and Figure 4.3 show the significant wave height and peak wave period roses, respectively, at TNWA-2, TNWB and SON. No roses are shown for F3 because there are no wave direction observations available from F3. The rose with the TNWA-2 data is smaller due to the data covering only about half of the month. There is an overall agreement between the TNWB and the SON roses. Given SON's location nearer the shore (cf. Figure 1.2), there are less waves from Southwest and the Eastern waves have due to refraction a more northern alignment at SON.
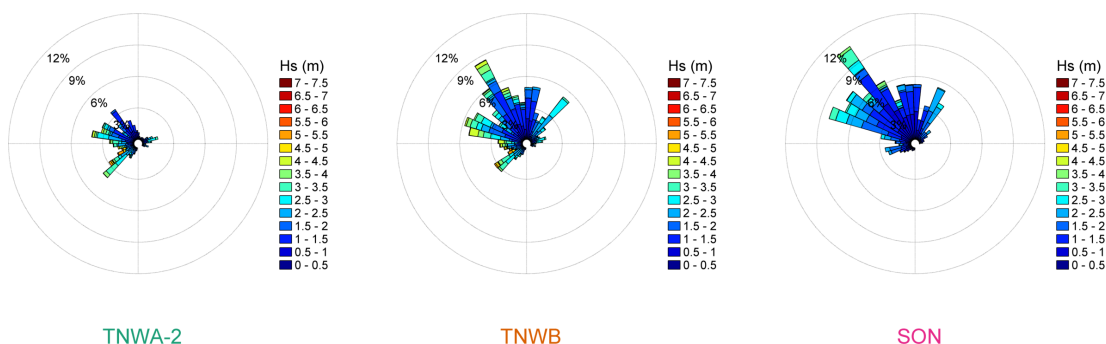
Figure 4.2: *Significant wave height roses (data from January 2021).*
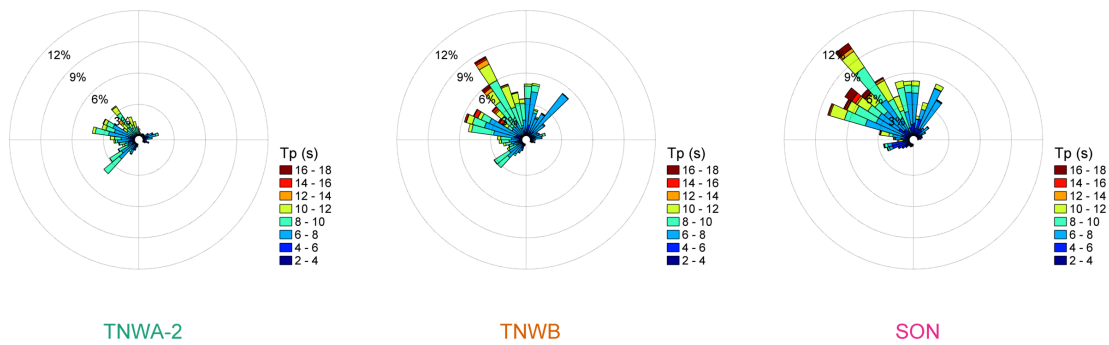
Figure 4.3: *Peak wave period roses (data from January 2021).*

4.2.2 Ten Noorden van de Waddeneilanden Buoy TNWA-2

Figures 4.4 and 4.5 show comparisons between TNWA observations and those at F3 and SON of H_s, T_p, mean wave period, $T_{m0,2}$, and mean wave direction, MWD (only SON, Figure 4.5). The correlation, root-mean-square error and bias statistics are printed in each of the figures.

As can be seen in the figures, the comparisons between TNWA-2 observations and those:

- at F3 are excellent in terms of significant and swell wave height, good in terms of mean wave period and poor in terms of peak wave period; and
- at SON are good in terms of significant and swell wave height and mean wave direction and poor in terms of mean and peak wave period.

The discrepancies between the SON and the TNWA-2 data occur mostly between the 20th and the 21st of January, when there is less energy reaching the shallower and closer to the shore location of SON (cf. Figure 1.2). Discrepancies in terms of peak wave period between the data from all locations are also expected given the discrete characteristics of the variable.

Deltares
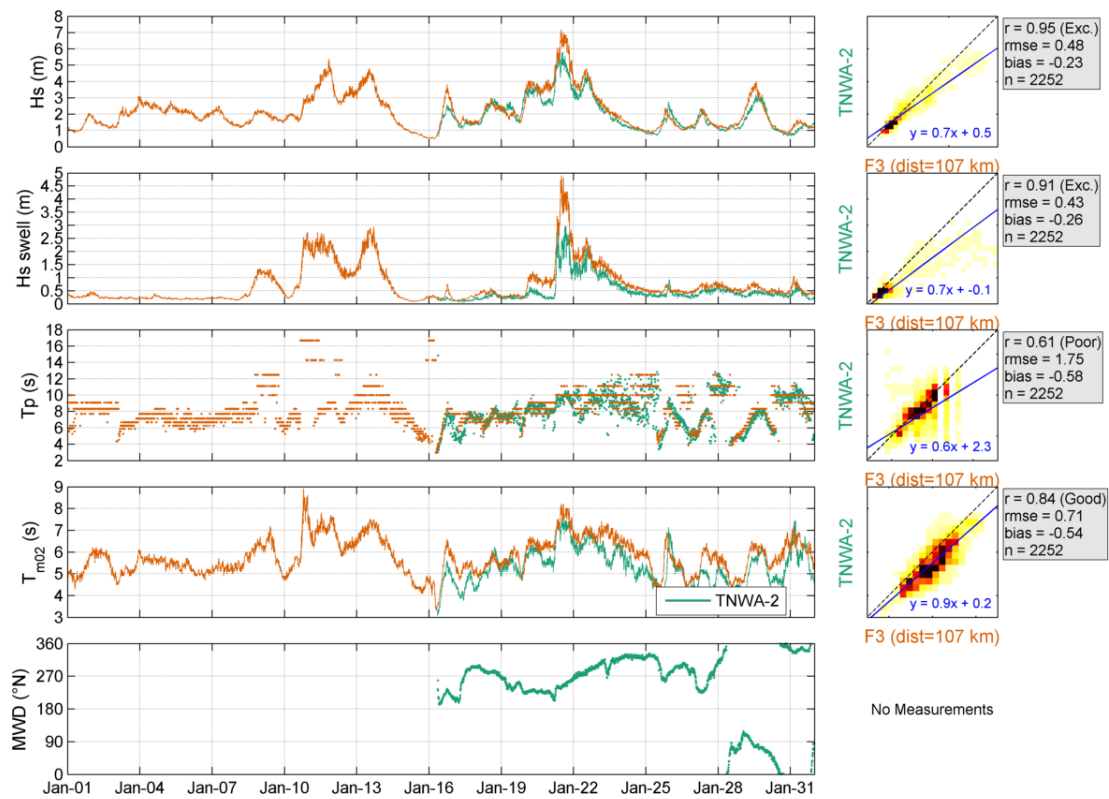
Figure 4.4: *Validation of TNWA-2 (data from January 2021) with F3 wave data. Left panels: Timeseries. Right panels: Density scatter (darker colours indicating higher data density).*
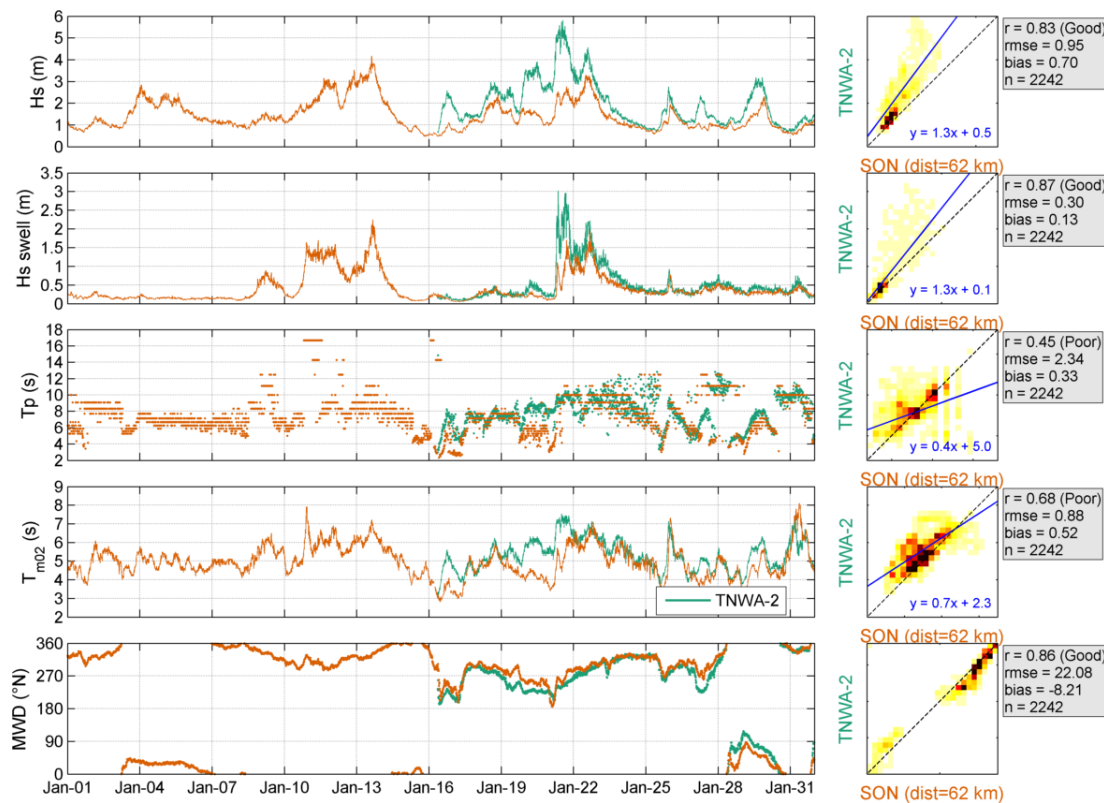
Figure 4.5: *Validation of TNWA-2 (data from January 2021) with SON wave data. Left panels: Timeseries. Right panels: Density scatter (darker colours indicating higher data density).*

4.2.3 Ten Noorden van de Waddeneilanden Buoy TNWB

Figures 4.6 and 4.7 show comparisons between TNWB observations and those at F3 and SON of H_s, T_p, mean wave period, $T_{m0,2}$, and mean wave direction, MWD (only SON, Figure 4.7). The correlation, root-mean-square error and bias statistics are printed in each of the figures.

As can be seen in the figures, the comparisons between TNWB observations and those:

- at F3 are excellent in terms of significant and swell wave height, good in terms of mean wave period and poor in terms of peak wave period; and
- at SON are excellent in terms of swell wave height and mean wave direction, good in terms of significant wave height, reasonable in terms of mean wave period and poor in terms of peak wave period.

As was the case in the validation of the TNWA-2 data, the discrepancies between the SON and the TNWB data occur mostly between the 20th and the 21st of January, when there is less energy propagating into SON.
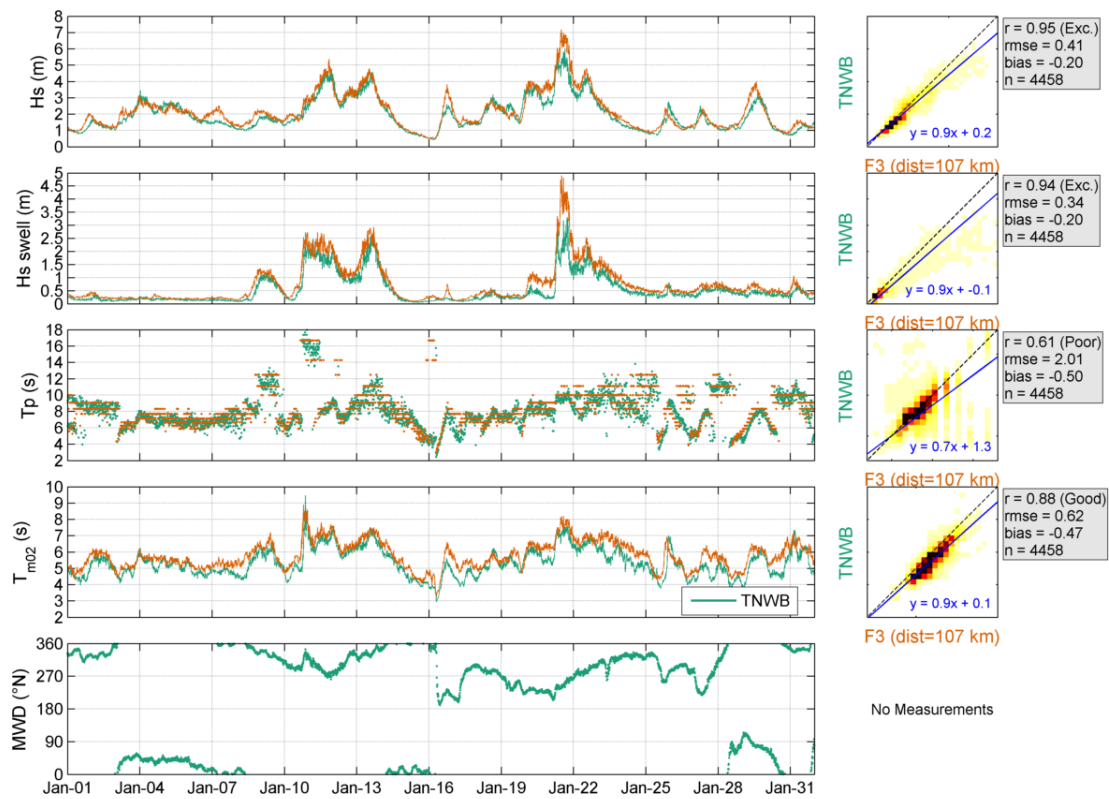
Figure 4.6: *Validation of TNWB (data from January 2021) with F3 wave data. Left panels: Timeseries. Right panels: Density scatter (darker colours indicating higher data density).*
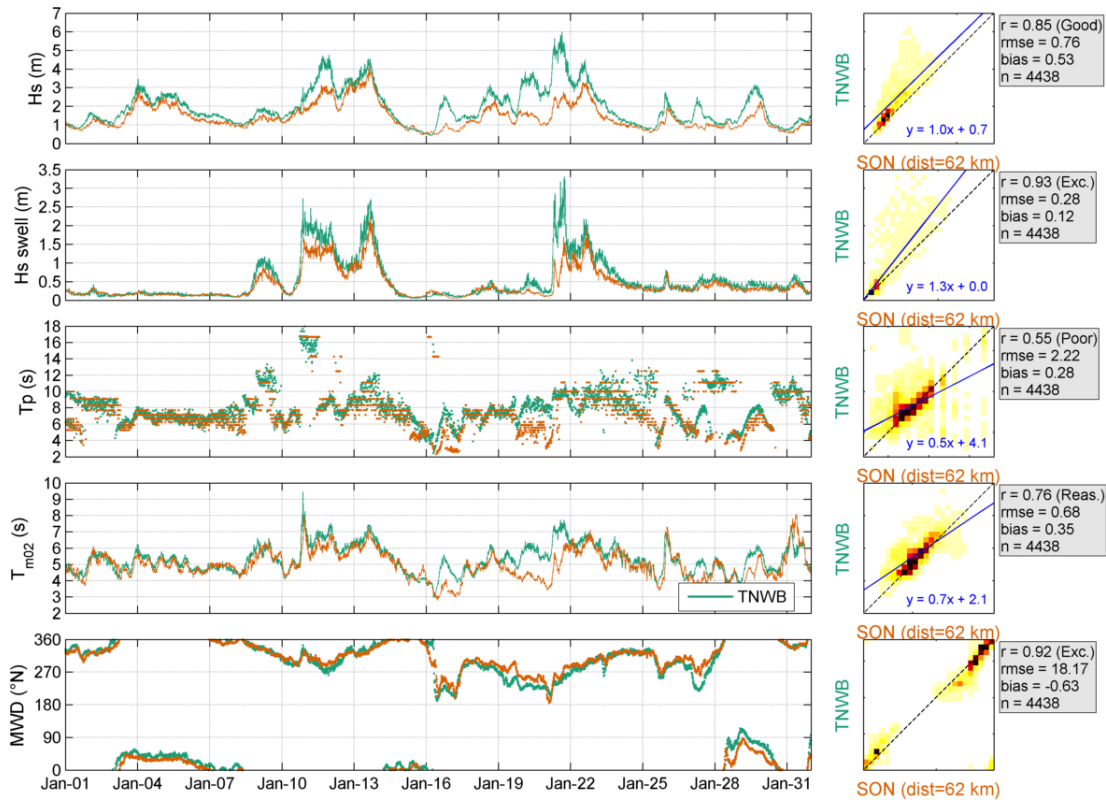
Figure 4.7: *Validation of TNWB (data from January 2021) with SON wave data. Left panels: Timeseries. Right panels: Density scatter (darker colours indicating higher data density).*

4.3 Summary and conclusions

The correlations between the buoy and the fixed station wave observations given in figures 4.4 to 4.5 and 4.6 to 4.7 are summarized in Table 4.2.

Table 4.2: *Statistical comparison between the TNWA-2 and TNWB buoy observations and those from the fixed stations.*

	TNWA-2		TNWB	
Station	F3	SON	F3	SON
$H_s\ r$ **(-)**	0.95	0.83	0.95	0.85
$H_s\ n$ **(-)**	2252	2242	4458	4438
$H_{sswell}\ r$ **(-)**	0.91	0.87	0.94	0.93
$H_{sswell}\ n$ **(-)**	2252	2242	4458	4438
$T_p\ r$ **(-)**	0.61	0.45	0.61	0.55
$T_p\ n$ **(-)**	2252	2242	4458	4438
$T_{m02}\ r$ **(-)**	0.84	0.68	0.88	0.76
$T_{m02}\ n$ **(-)**	2252	2242	4458	4438

Based on a) the comparisons between the data from the buoys, which are excellent for all parameters, except as expected those depending strongly on the sampling variability (randomness of the sea surface elevation) and discreteness of the wave spectra (T_p, $T_{m02swell}$ and MWD_{swell}, cf. Table 4.1), and b) the validation of the data against the platform observations, in which mismatches can be explained by local effects, spatial variations and again discreteness of the wave spectra, it can be concluded that the accuracy of the TNW buoy wave data is high.

5 Temperature

During this deployment period air and surface water temperatures are measured at both buoys and the bottom water temperature by both WLS, but the availability of the bottom temperature data from TNWB is only 1.3% (cf. Figure 2.1).

5.1 Overview

Figure 5.1 shows the observed air and water temperature and their differences. All signals align.

Figure 5.1 also show that the bottom temperature observations are generally higher than those at the surface. However, the temperature sensors in the WLS have not been calibrated, the bottom temperature can thus be biased and are given solely for illustration of the bottom temperature temporal variations, which are in principle measured accurately.
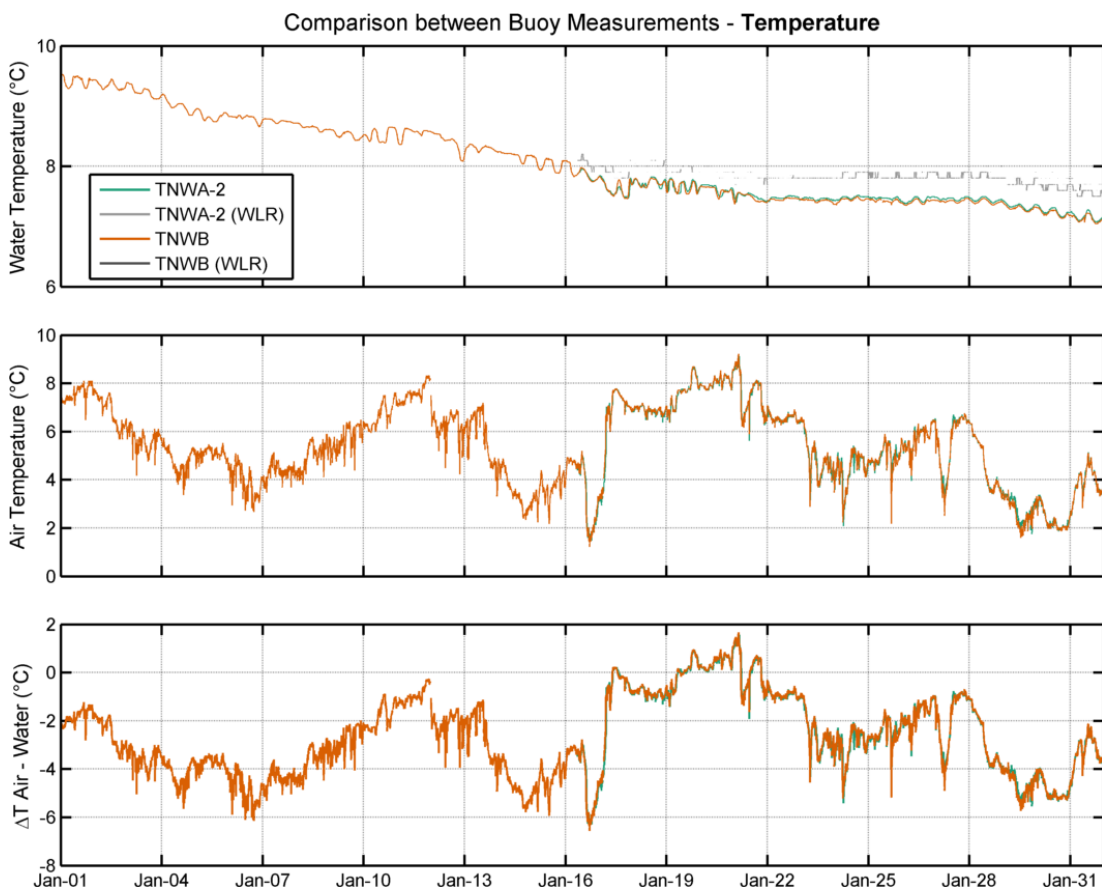
Figure 5.1: *Temperature difference measured at LiDAR buoys (data from January 2021).*

5.2 Validation

The comparisons between fixed station measurements and the TNW data are presented in Section 5.2.1 (water temperature) and in Section 5.2.2 (air temperature).

5.2.1 Water Temperature

A timeseries comparison between the observations from both buoys and sensors and the fixed stations is presented in Figure 5.2. The water temperature observations from the fixed stations are all surface temperatures. Figure 5.2 shows a few outliers in the measurements at K13, which have not been removed. Furthermore, the figure shows that during this period there are some spatial gradients in the temperature with the coolest temperatures being observed at the nearshore SON location, where also the largest daily variations are observed.
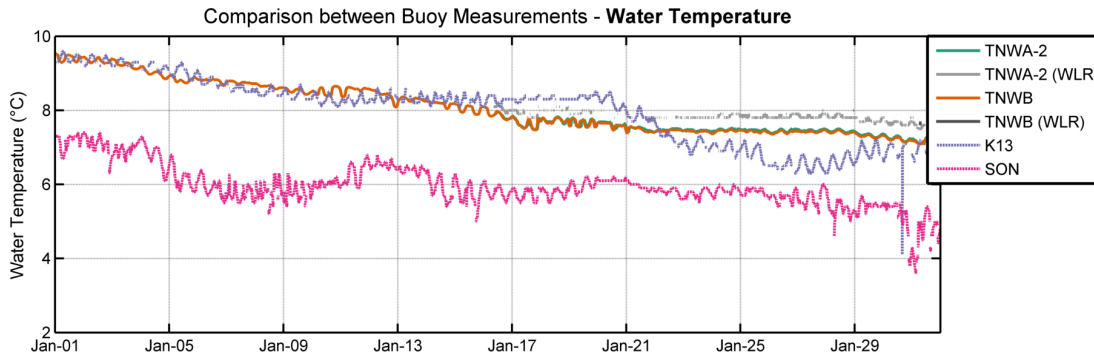
Figure 5.2: *Water temperature measurements from all locations (data from January 2021).*

A direct comparison of the measured surface water temperature at TNWA-2 and TNWB against the fixed stations is provided in Figure 5.3 and Figure 5.4, respectively. As could already be inferred from the spatial variations shown in Figure 5.2 in particular after the 16th of January, when the TNWA-2 data are available, there is a poor agreement between the TNWA-2 and the K13 and SON data. Given that the TNWB data cover the full period and at the first half of the month the TNWB temperature are aligned with those at K13, the agreement between the TNWB and the K13 data is good and between the TNW and the SON data is reasonable.
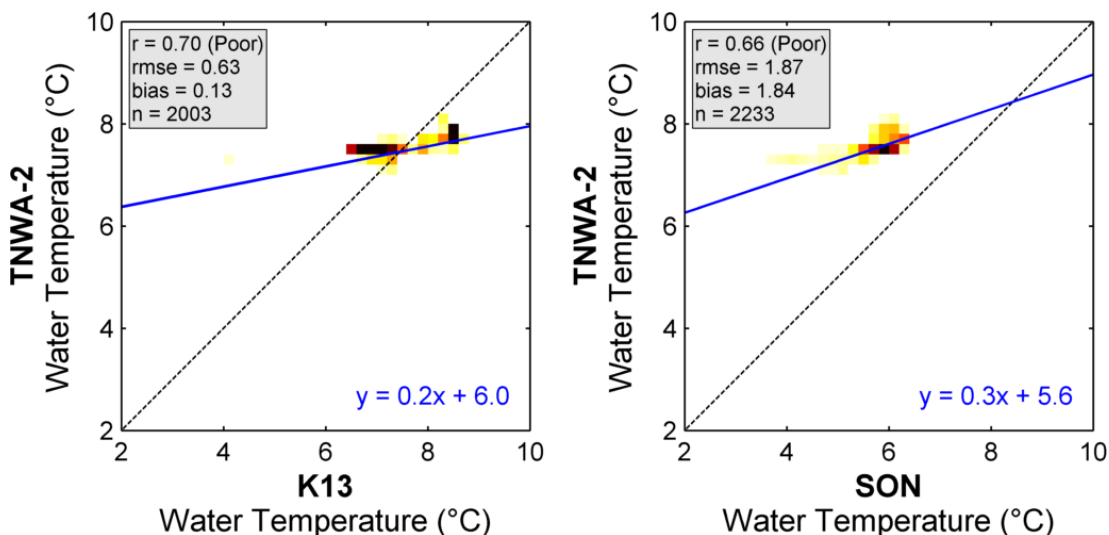
Figure 5.3: *Surface water temperature comparison at TNWA-2 (data from January 2021).*
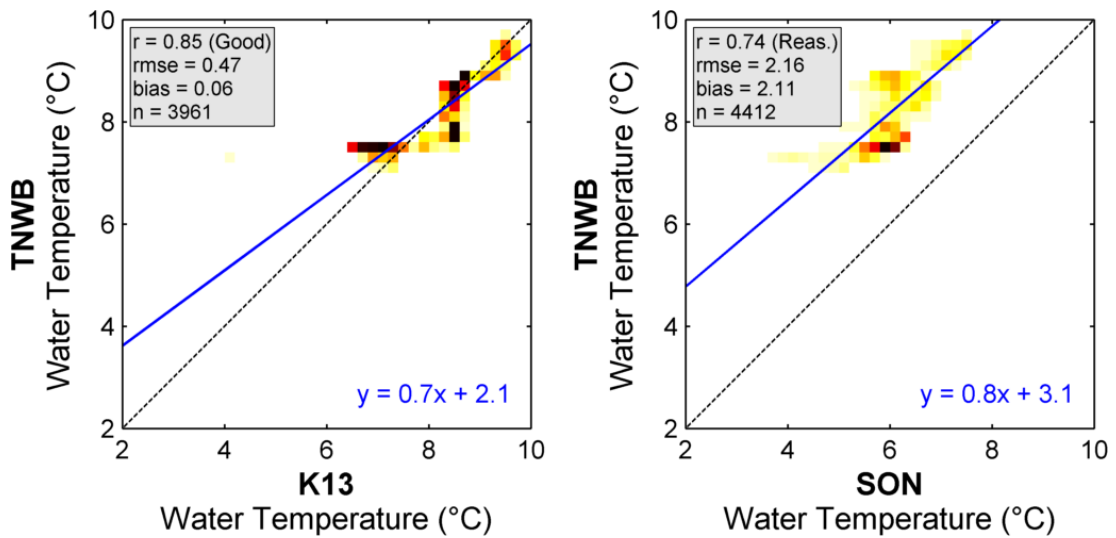
Figure 5.4: Surface water temperature comparison at TNWB (data from January 2021).

5.2.2 Air Temperature

A timeseries comparison of the measured air temperature between the observations at TNWA-2 and TNWB and those at BG is provided in Figure 5.5. All datasets align. A direct comparison of the measured air temperature at TNWA-2 and TNWB and the observations at BG is provided in Figure 5.6. As could also be seen in Figure 5.5, the agreements are all excellent. Note that the stepwise timeseries of BG is due to the coarse (1 °C) discretization of the available raw measurements.
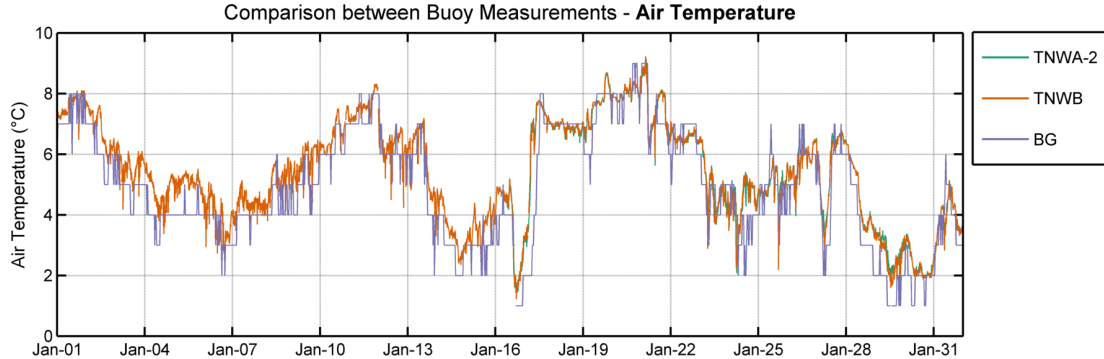
Figure 5.5: Air temperature measurements from all locations (data from January 2021).
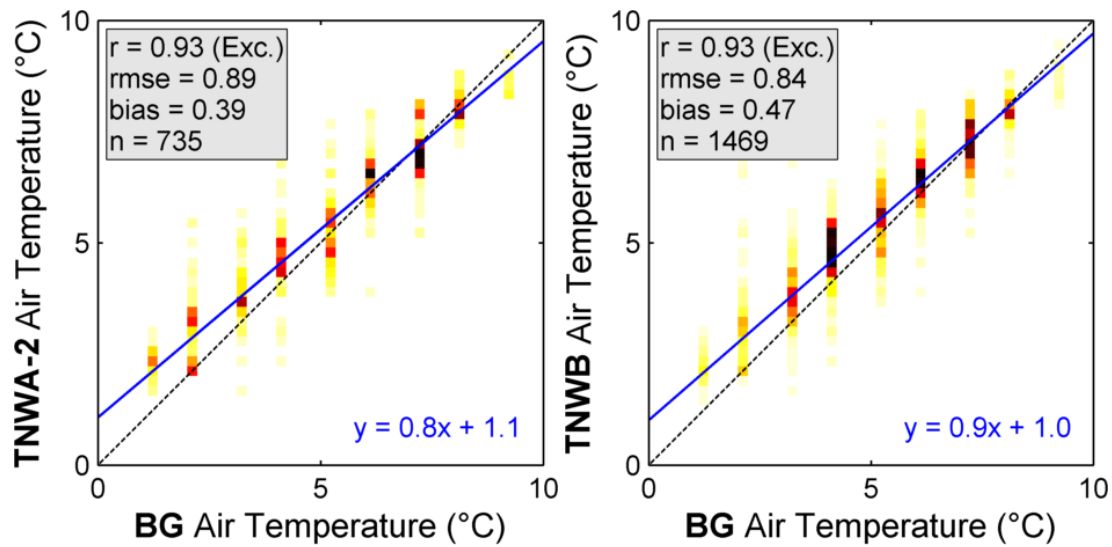
***Figure 5.6:** Air temperature comparison at TNWA-2 (left panel) and TNWB (right panel). Data from January 2021.*

5.3 Conclusions

The validation of the temperature data shows that there are large spatial variations in the water temperatures during this period and a general agreement between TNW and fixed station air temperature observations.

6 Air Pressure

6.1 Overview

An overview of the available air pressure measurements from TNWA-2, TNWB, L91, K13, and F3 is shown in Figure 6.1. The signals show near-identical variations in time, as expected, given their proximity with respect to macro-atmospheric forcings. The figure also shows that there is most of the time an offset between the L91 data and the data from the other stations, which is not as expected and can be seen as an indication of biases in the L91 data.
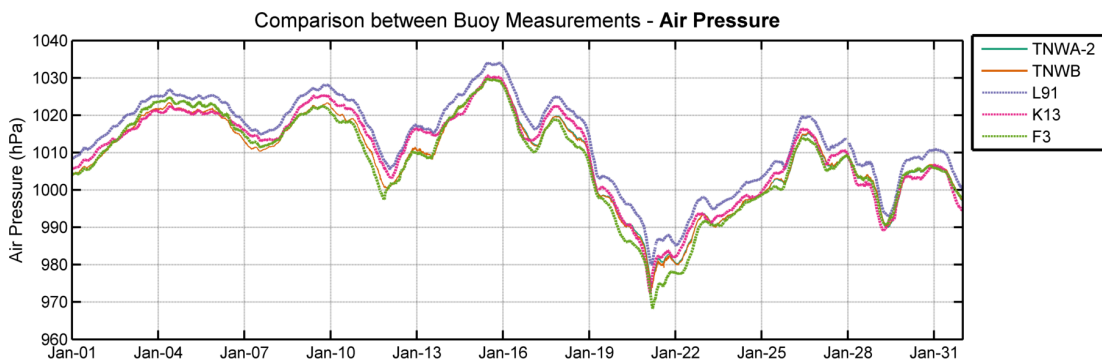
Figure 6.1: *Air pressure measurements from all locations.*

6.2 Validation

A direct comparison of the measured air pressure at TNWA-2 (TNWB) against those of the fixed stations is given in Figure 6.2 (Figure 6.3). As could already be inferred from the variations shown in Figure 6.1, the agreements are all excellent and there is a bias of about 4 hPa between the L91 and the TNW data.
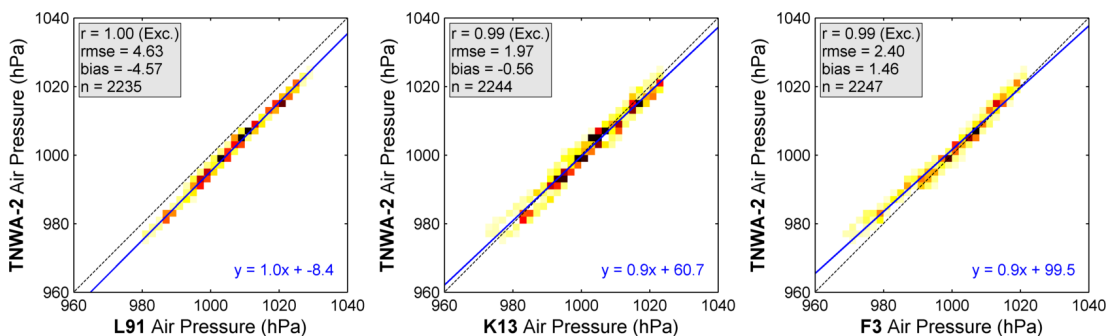
Figure 6.2: *Air pressure comparison at TNWA-2 (data from January 2021).*
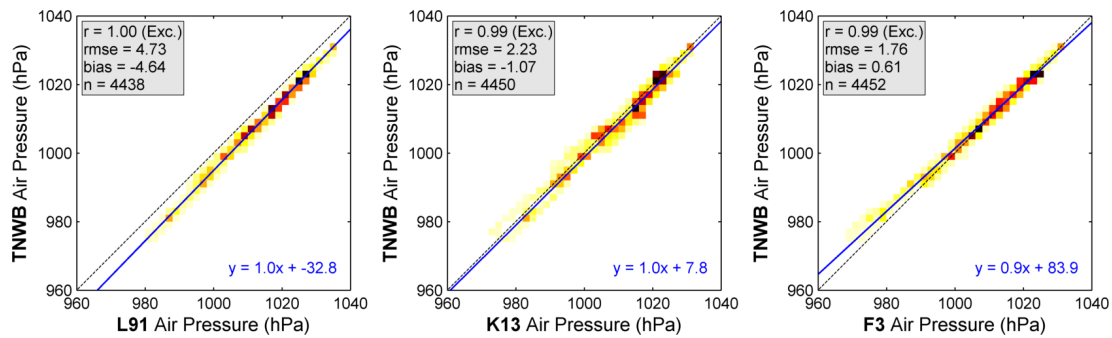
***Figure 6.3:** Air pressure comparison at TNWB (data from January 2021).*

6.3 Conclusions

The validation of the air pressure data shows, as expected given their proximity in terms of macro-atmospheric forcings, an excellent agreement between the TNW observations and those from the fixed stations.

7 Water Level

7.1 Overview

Still (or total) water levels above Lowest Astronomical Tide (LAT) are determined by Fugro from the WLS pressure measurements. During this validation period water level observations are available from the 16th from the WLS at TNWA-2 and from the 25th from the WLS at TNWB (with many gaps, cf. Figure 2.1). The available data are shown in Figure 7.1. The figure shows a good alignment and an offset between the TNWA and the TNWB water levels, the offset is probably due to uncertainties in the applied LAT reference level.
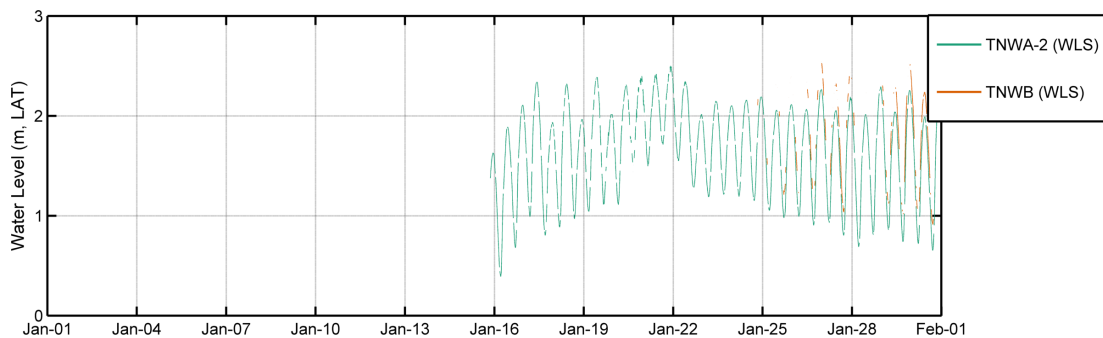
Figure 7.1: *TNW still water levels.*

7.2 Description and validation

The nature of the tidal wave propagation in the North Sea limits the ability to validate with nearby fixed platforms (i.e. distinct tidal amplitudes and phases). Therefore, the validation of the TNWA-2 water level data can only be done against model data. The 3D DCSM-FM described in Appendix A has been run purposely for the validation of the TNW water levels and currents (given in the next chapter) and results output at the TNW locations.

Figure 7.2 shows the comparisons between the still water level observations from TNW and the corresponding 3D DCSM-FM model results. The figure shows that there is an excellent agreement between the signals. The figure also shows that there is an offset of 1.50 m between the TNWA-2 and the DCSM-FM water levels and an offset of 1.78 m between the TNWB and the DCSM-FM water levels, this is to some extent due to the observations being given with reference to LAT and the model results with reference to Mean Sea Level (MSL) but also some uncertainty in these vertical references.
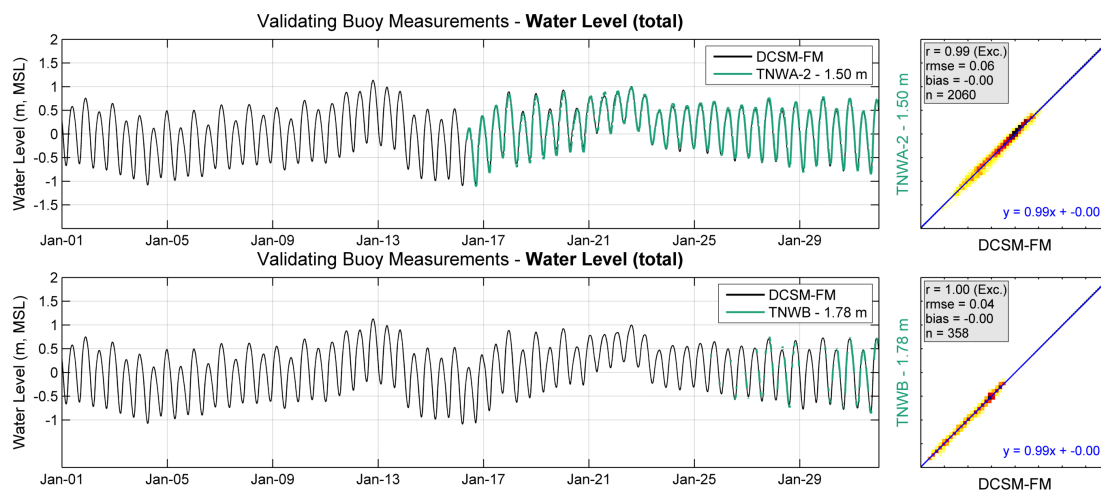
Figure 7.2: *TNWA-2 (top panel) and TNWB (bottom panel) and 3D DCSM-FM still water levels.*

7.3 Conclusions

As shown above, although in particular from TNWB the water level data availability is low, there is a high correlation between the model and WLS TNW water levels.

8 Currents

8.1 Ten Noorden van de Waddeneilanden description and intercomparison

During this period there are currents observations available from TNWA-2 (from the 16th) and from TNWB (from the 25th). The current speed and direction are measured at depths 3 to 38 m with a spacing of 1 m at TNWA-2 and TNWB. Even though the observations close to the bottom are of lower quality and not always available due to the water level variations, in this report we still consider the current velocity data down to a (near bottom) depth of 36 m.

To get a full overview of the data two movies were created with the time evolution of vertical current profiles at TNWA-2 (see here) and TNWB (see here).

Figure 8.1 shows the timeseries of the observed surface (3 m) current speeds, with the corresponding roses being given in Figure 8.2. Given that the TNWA-2 data covers a longer period, the roses are not comparable. Figures 8.3 and 8.4 show the observed current speeds and directions, respectively, as a function of depth. As can be seen in the figures, the currents in TNW are predominantly tidally driven, with an alignment close to East-West and with the stronger currents being towards the East.
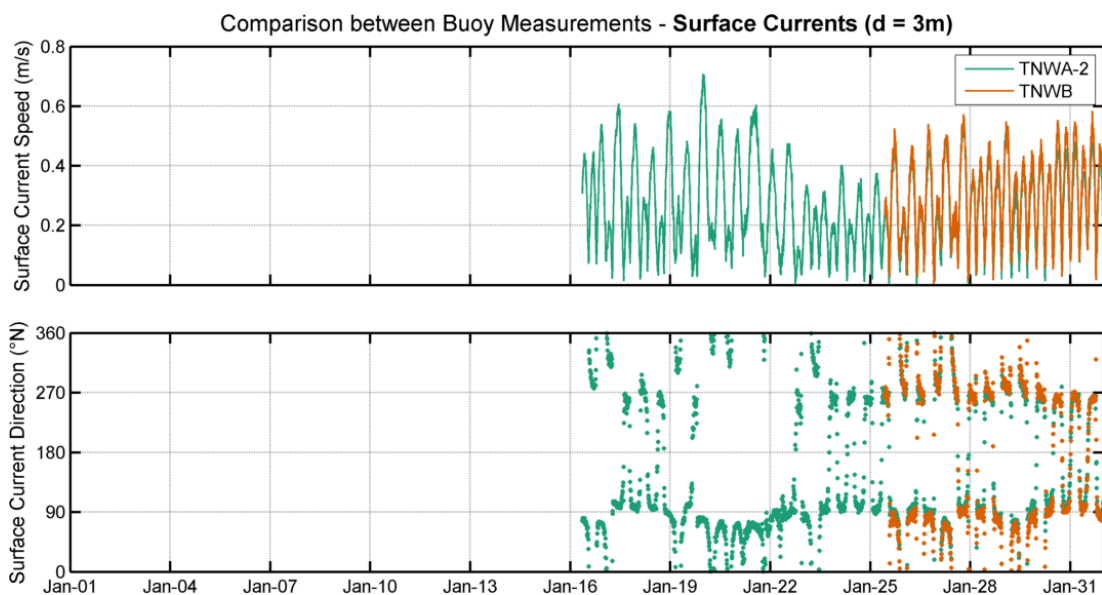
Figure 8.1: *Surface currents at each buoy. Left panels: Timeseries. The oceanographic convention is used for the current directions, so all current directions are going to, clockwise from North.*

Comparison between Buoy Measurements - **Surface Currents (d = 3m)**
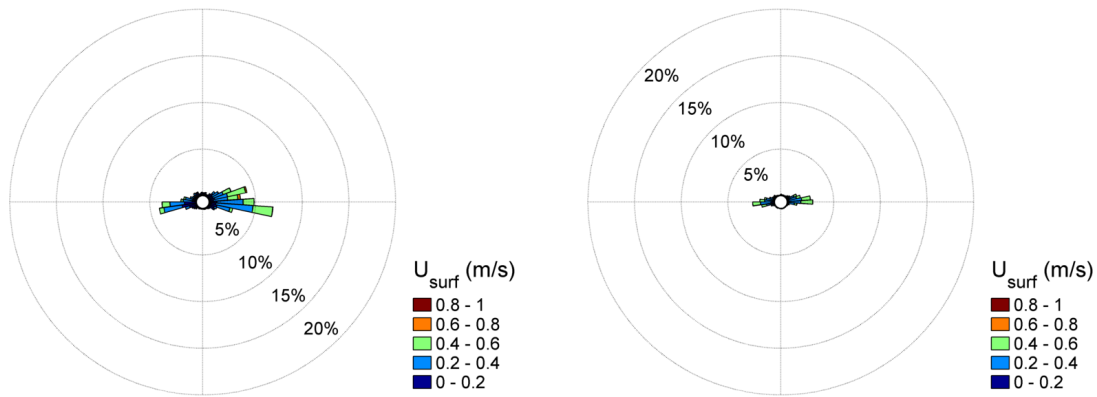
TNWA-2

TNWB

Figure 8.2: *Surface (3 m) current roses (bin width 8°) at each buoy (data from January 2021). The TNWA-2 data are only available from 16-01-2021 and the TNWB data from 25-01-2021. The current direction is the direction the piles point to away from the centre of the rose.*
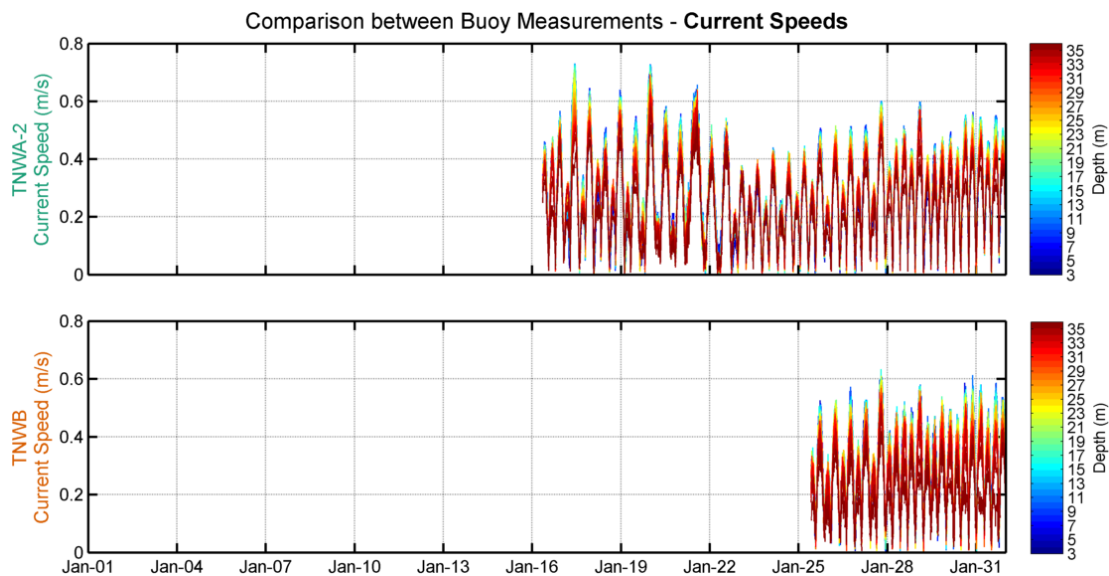
Figure 8.3: *Current speeds (by depth) at each buoy. Left panels: Timeseries.*
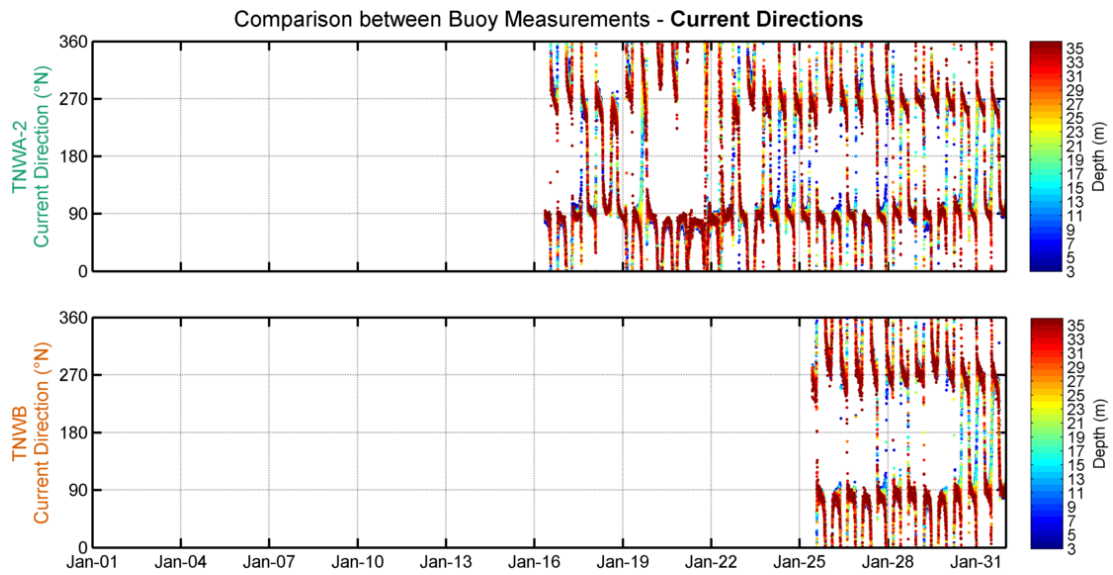
Figure 8.4: *Current directions (by depth) at each buoy (from January 2021). Left panels: Timeseries. The oceanographic convention is used for the current directions, so all current directions are going to clockwise from North.*

Figure 8.5 shows all observed vertical current profiles (grey lines) and the mean profile (red line). Note that the TNWB data cover a shorter period, nevertheless, the shown mean profile of TNWA-2 and TNWB observations appears realistic.
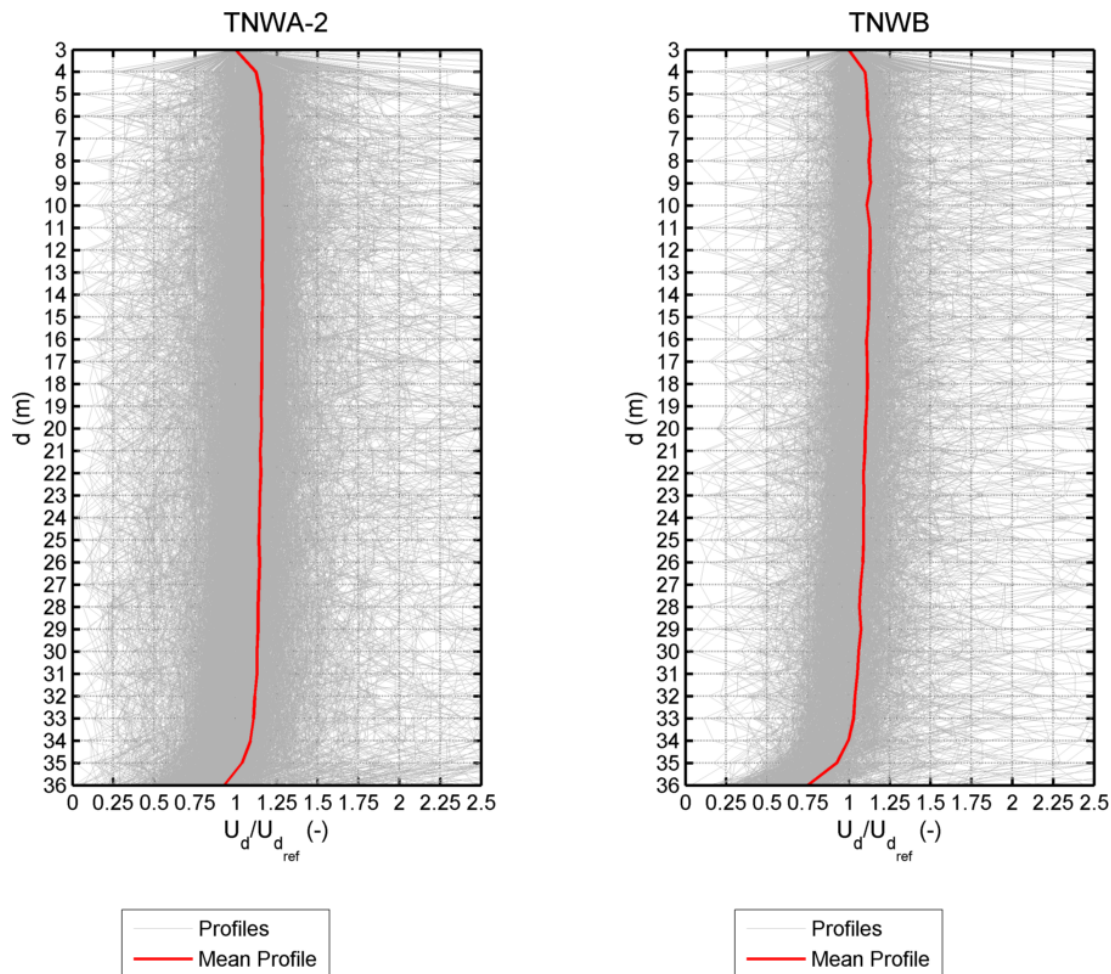
Figure 8.5: *Normalized (with relation to the 3 m level) TNW current speed vertical profile (January 2021). The x-axis has a fixed lower limit of 0 and upper limit of 2.5 for readability.*

In order to further quantify the differences between the currents observed by two buoys, the slope, bias, correlations and square correlations between the TNWA-2 and TNWB current speed observations at all depths and the bias, correlations and square correlations between the TNWA-2 and TNWB current direction observations at all depths have been computed and are given in Table 8.1. The correspondence between the data is down to a level of 34 m excellent in terms of current speed and poor in terms of current direction. The lower current direction correlations can to a large extent be explained by the nature and variability of the current direction signal. Due to the rotating nature of the currents, especially when they rapidly rotate towards offshore (directions close to 350) the timing can be off. This occurs, however, during short time periods and mostly when the current speeds are low. To demonstrate this, Table 8.2 shows the current direction statistics computed considering only current speeds above 0.1 m/s. As can be seen in the table, the correlations between the current directions are then higher.

Deltares

Table 8.1: Statistical comparison between LiDAR buoy current measurements with depth.

Depth (m)	Current Speed					Current Direction			
	r^2 (-)	r (-)	Bias (m/s)	Symm. Slope (-)	n (-)	r^2 (-)	r (-)	Bias (°)	n (-)
3	0.93	0.97	0.02	1.09	944	0.40	0.63	-1.7	944
4	0.95	0.97	0.01	1.03	943	0.40	0.63	-2.1	943
5	0.95	0.98	0.01	1.02	944	0.41	0.64	-3.0	944
6	0.95	0.98	0.01	1.01	944	0.44	0.66	-2.4	944
7	0.95	0.98	0.01	1.02	944	0.49	0.70	-3.2	944
8	0.95	0.97	0.01	1.01	944	0.47	0.69	-3.2	944
9	0.95	0.98	0.01	1.01	944	0.53	0.73	-2.6	944
10	0.95	0.97	0.01	1.01	944	0.47	0.69	-2.5	944
11	0.95	0.98	0.01	1.01	944	0.48	0.69	-3.2	944
12	0.95	0.97	0.01	1.01	944	0.47	0.68	-2.7	944
13	0.96	0.98	0.01	1.01	944	0.46	0.68	-2.6	944
14	0.95	0.98	0.01	1.02	944	0.50	0.71	-2.4	944
15	0.95	0.98	0.01	1.01	944	0.42	0.65	-2.8	944
16	0.96	0.98	0.01	1.01	944	0.46	0.68	-2.2	944
17	0.95	0.98	0.01	1.01	944	0.43	0.66	-2.5	944
18	0.95	0.98	0.01	1.01	944	0.45	0.67	-2.7	944
19	0.95	0.97	0.01	1.01	944	0.46	0.68	-2.7	944
20	0.95	0.97	0.01	1.01	944	0.45	0.67	-3.4	944
21	0.96	0.98	0.01	1.01	944	0.45	0.67	-2.7	944
22	0.95	0.98	0.00	1.01	944	0.41	0.64	-3.1	944
23	0.95	0.97	0.00	1.01	944	0.41	0.64	-2.6	944
24	0.95	0.98	0.01	1.01	944	0.48	0.69	-2.6	944
25	0.94	0.97	0.01	1.01	944	0.40	0.63	-2.3	944
26	0.95	0.97	0.00	1.01	944	0.46	0.67	-2.3	944
27	0.95	0.97	0.00	1.00	944	0.43	0.66	-3.1	944
28	0.94	0.97	0.00	1.00	944	0.49	0.70	-3.1	944
29	0.94	0.97	0.00	1.00	944	0.45	0.67	-2.3	944
30	0.94	0.97	0.00	1.00	944	0.48	0.69	-3.3	944
31	0.94	0.97	0.00	1.00	944	0.49	0.70	-2.2	944
32	0.93	0.97	0.00	1.00	944	0.55	0.74	-3.0	944
33	0.93	0.96	-0.00	0.99	944	0.53	0.73	-2.3	944
34	0.91	0.96	-0.00	0.97	944	0.57	0.76	-2.5	944
35	0.86	0.93	-0.02	0.93	944	0.54	0.73	-2.5	944
36	0.76	0.87	-0.03	0.85	944	0.38	0.62	-2.6	944

Table 8.2: *Statistical comparisons, with depth and considering only speeds above 0.1 m/s, between LiDAR buoy current direction measurements, .*

Depth (m)	r^2 (-)	r (-)	Bias (°)	n (-)
	Current Direction			
3	0.58	0.76	-3.2	807
4	0.61	0.78	-2.6	833
5	0.59	0.77	-2.5	833
6	0.62	0.79	-2.5	832
7	0.60	0.78	-2.7	836
8	0.61	0.78	-2.6	835
9	0.58	0.76	-2.4	839
10	0.59	0.77	-2.5	835
11	0.57	0.75	-2.2	835
12	0.52	0.72	-2.5	825
13	0.51	0.71	-2.6	833
14	0.54	0.73	-2.4	836
15	0.52	0.72	-2.4	831
16	0.55	0.74	-2.3	823
17	0.50	0.71	-2.7	821
18	0.48	0.69	-2.3	824
19	0.50	0.71	-2.6	824
20	0.52	0.72	-2.8	819
21	0.49	0.70	-2.9	819
22	0.53	0.73	-2.4	822
23	0.47	0.69	-2.6	819
24	0.50	0.71	-2.6	817
25	0.53	0.73	-2.2	814
26	0.54	0.74	-2.1	820
27	0.55	0.74	-2.7	813
28	0.58	0.76	-2.8	816
29	0.56	0.75	-2.4	817
30	0.52	0.72	-2.5	818
31	0.56	0.75	-2.5	825
32	0.58	0.76	-2.5	823
33	0.59	0.77	-2.4	826
34	0.60	0.78	-2.3	814
35	0.55	0.74	-2.3	800
36	0.33	0.57	-2.9	754

8.2   Validation

The validation of the measured currents is completed with data from Deltares 3D Dutch Continental Shelf Model-Flexible Mesh (3D DCSM-FM) described in Appendix A. Given the lack of 3D current data from other sources, 3D DCSM-FM has been run purposely for this validation.

8.2.1 Model results in Ten Noorden van de Waddeneilanden

The resolution of 3D DCSM-FM in the area of the buoys is about 900 m x 900 m and so the bottom schematization of the model does not fully describe the very fine-scale bottom variations in the area (cf. Figure 1.1). Therefore, the model results are expected to vary more smoothly than the true current variations between the two buoy locations.

Table 8.3 shows the slopes, biases and correlations between the current speed model results at TNWA-2 and TNWB and the correlations and biases between the current direction model results at TNWA-2 and TNWB considering the same depth levels and timestamps as those of the buoy observations given in Table 8.1. Note that the model output at TNWA-2 and TNWB is due to the resolution of the model from adjacent grid points. As expected, the agreement between the data is excellent both in terms of current speed and direction. Note that although the correlations between the directions are lower than those between the speeds, they are higher than those obtained between the observed current directions, since the model is not affected in the same way as the buoy by the rapid changes in current direction.

Table 8.3: *Statistical comparison between the 3D DCSM-FM results at the buoy locations and at the timestamps at which the buoy data are valid with depth.*

Depth (m)	Current Speed				Current Direction		
	r (-)	Bias (m/s)	Symm. Slope (-)	n (-)	r (-)	Bias (°)	n (-)
3	0.99	-0.00	0.99	944	0.96	-0.2	944
4	0.99	-0.00	0.99	943	0.96	-0.0	943
5	0.99	-0.00	0.99	944	0.96	0.1	944
6	0.99	-0.00	0.99	944	0.96	0.3	944
7	0.99	-0.00	0.99	944	0.96	0.3	944
8	0.99	-0.00	0.99	944	0.95	0.3	944
9	0.99	-0.00	0.99	944	0.95	0.3	944
10	0.99	-0.00	0.99	944	0.95	0.2	944
11	0.99	-0.00	0.99	944	0.95	0.1	944
12	0.99	-0.00	0.99	944	0.96	-0.2	944
13	0.99	-0.00	0.99	944	0.96	-0.2	944
14	1.00	-0.00	0.99	944	0.95	-0.1	944
15	1.00	-0.00	0.99	944	0.95	-0.1	944
16	1.00	-0.00	0.99	944	0.97	0.0	944
17	1.00	-0.00	0.99	944	0.97	-0.0	944
18	1.00	-0.00	0.99	944	0.98	0.1	944
19	1.00	-0.00	0.99	944	0.98	0.1	944
20	1.00	-0.00	0.99	944	0.99	0.2	944
21	1.00	-0.00	1.00	944	0.99	0.1	944
22	1.00	-0.00	1.00	944	0.99	0.2	944
23	1.00	-0.00	1.00	944	0.99	0.2	944
24	1.00	-0.00	1.00	944	0.99	0.4	944
25	1.00	-0.00	1.00	944	0.99	0.2	944
26	1.00	-0.00	1.00	944	0.99	0.3	944
27	1.00	0.00	1.00	944	0.99	0.3	944
28	1.00	0.00	1.00	944	0.99	0.3	944
29	1.00	0.00	1.00	944	0.99	0.3	944
30	1.00	0.00	1.00	944	0.99	0.3	944
31	0.99	0.00	1.00	944	0.99	0.3	944
32	0.99	0.00	1.00	944	0.99	0.3	944
33	0.99	0.00	1.00	944	0.99	0.4	944
34	0.99	0.00	1.00	944	0.99	0.4	944
35	0.99	0.00	1.00	944	0.99	0.4	944
36	0.99	0.00	1.00	944	0.99	0.4	944

8.2.2 Ten Noorden van de Waddeneilanden Buoy TNWA-2

A direct comparison between the 3D DCSM-FM surface current (d = 3 m) at TNWA-2 and the buoy observations is given in Figure 8.6 in terms of timeseries and Figure 8.7 in terms of roses. The same comparisons are shown in Figure 8.8 in terms of timeseries and Figure 8.9 in terms of roses for the current at 23 m (about 60% down the water column). At both levels the agreements are good in terms of current speed and poor in terms of current direction. Furthermore, the roses show more directional spreading in the observations and a larger west-east current asymmetry, with a higher predominance of currents towards the East in the observations. Table 8.4 shows the error statistics between the current speed and direction of the model at TNWA-2 and the TNWA-2 data at the observed levels from a depth of 3 m to 36 m. In terms of current speed the agreements are good at all levels, except for the lower level where they are acceptable. In terms of current direction the agreements are poor at all levels.
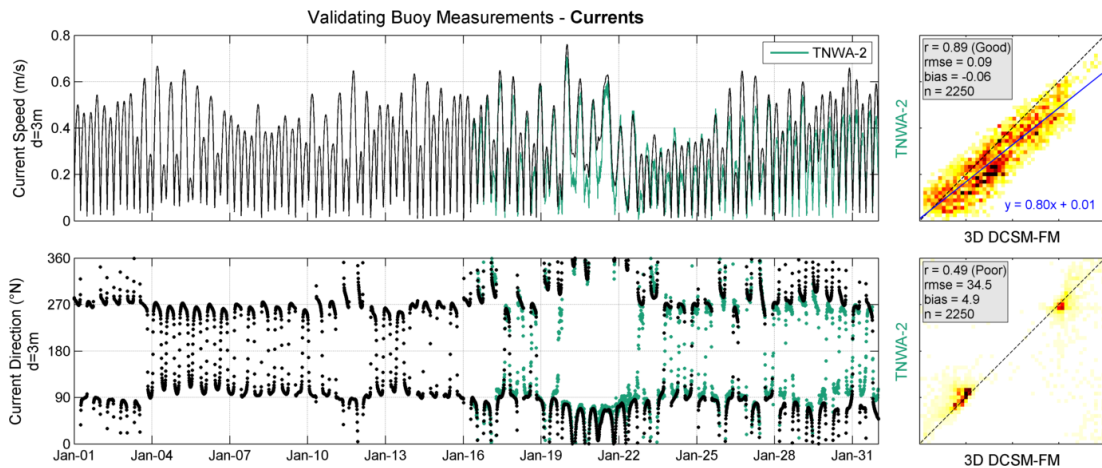
Figure 8.6: *Surface (d=3 m) current comparison at TNWA-2 (data from January 2021).*

Figure 8.7: *Buoy and 3D DCSM-FM roses (bin width 8°) of the surface (3 m) current velocity at TNWA-2 (data from January 2021. The current direction is the direction the piles point to away from the centre of the rose.*

Figure 8.8: *Current comparison at depth of 23 m TNWA-2 (data from January 2021.*

TNWA-2 comparison between buoy and 3D DCSM-FM currents (d = 23 m)
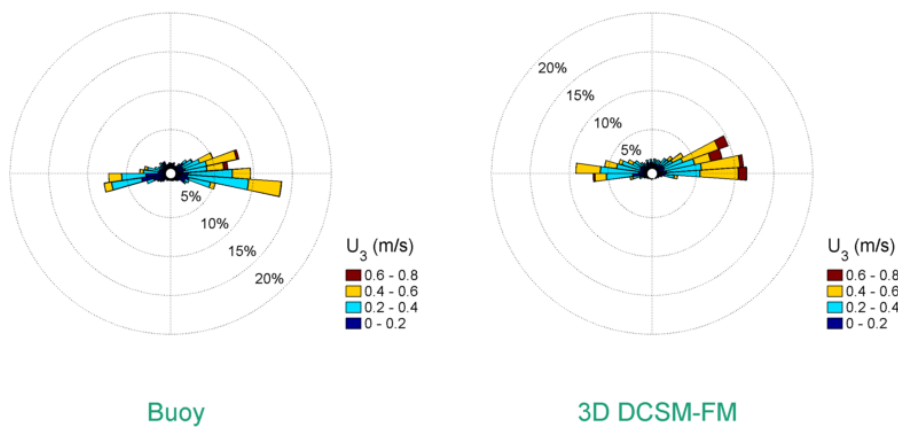

Buoy   3D DCSM-FM

Figure 8.9: *Buoy and 3D DCSM-FM roses (bin width 8°) of the 23 m current velocity at TNWA-2 (data from January 2021). The current direction is the direction the piles point to away from the centre of the rose.*
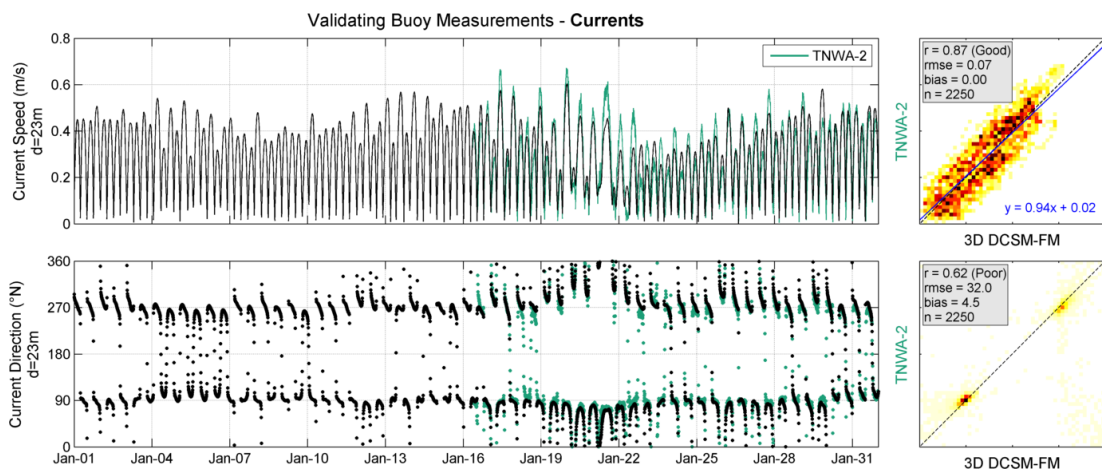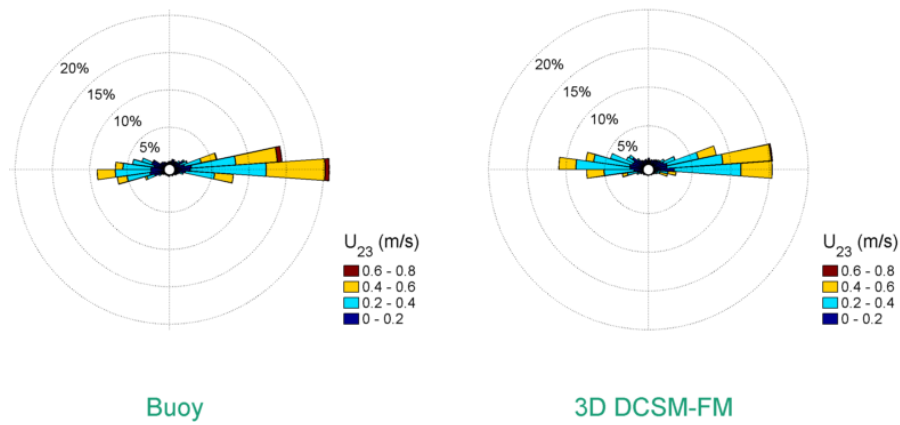
Table 8.4: *Statistical comparison between the 3D DCSM-FM results with TNWA-2 with depth.*

Depth (m)	Current Speed				Current Direction		
	r (-)	Bias (m/s)	Symm. Slope (-)	n (-)	r (-)	Bias (°)	n (-)
3	0.89	-0.06	0.83	2250	0.49	4.9	2250
4	0.89	-0.03	0.92	2250	0.49	3.8	2250
5	0.89	-0.02	0.94	2250	0.50	4.8	2250
6	0.89	-0.02	0.95	2250	0.49	5.2	2250
7	0.89	-0.02	0.96	2250	0.51	5.1	2250
8	0.88	-0.02	0.96	2250	0.49	4.8	2250
9	0.89	-0.02	0.96	2250	0.49	4.9	2250
10	0.88	-0.01	0.97	2249	0.48	4.5	2249
11	0.88	-0.01	0.97	2250	0.47	4.5	2250
12	0.88	-0.01	0.98	2250	0.48	4.0	2250
13	0.88	-0.01	0.98	2250	0.47	3.9	2250
14	0.88	-0.01	0.99	2250	0.51	3.3	2250
15	0.88	-0.01	0.99	2250	0.52	3.7	2250
16	0.88	-0.01	1.00	2250	0.54	3.7	2250
17	0.88	-0.01	1.00	2250	0.54	3.1	2250
18	0.88	-0.00	1.00	2250	0.57	3.9	2250
19	0.88	-0.00	1.01	2250	0.58	4.0	2250
20	0.88	-0.00	1.01	2250	0.59	4.2	2250
21	0.87	-0.00	1.02	2250	0.60	3.9	2250
22	0.87	-0.00	1.01	2250	0.63	4.7	2250
23	0.87	0.00	1.02	2250	0.62	4.5	2250
24	0.87	0.00	1.02	2250	0.63	4.3	2250
25	0.86	0.00	1.03	2250	0.60	4.0	2250
26	0.86	0.00	1.03	2250	0.64	5.4	2250
27	0.85	0.00	1.04	2250	0.62	5.5	2250
28	0.85	0.00	1.03	2250	0.64	5.0	2250
29	0.84	0.01	1.05	2250	0.63	5.2	2250
30	0.84	0.01	1.04	2250	0.64	5.0	2250
31	0.83	0.01	1.05	2250	0.64	5.0	2250
32	0.83	0.01	1.04	2250	0.64	4.7	2250
33	0.82	0.01	1.06	2250	0.63	5.1	2250
34	0.81	0.00	1.04	2250	0.63	3.8	2250
35	0.80	0.01	1.04	2250	0.62	4.2	2250
36	0.75	-0.02	0.94	2250	0.48	4.6	2250

8.2.3 Ten Noorden van de Waddeneilanden Buoy TNWB

A direct comparison between the 3D DCSM-FM surface current (d = 3 m) at TNWB and the buoy observations is given in Figure 8.10 in terms of timeseries and Figure 8.11 in terms of roses. The same comparisons are shown in Figure 8.12 in terms of timeseries and Figure 8.13 in terms of roses for the current at 23 m (about 60% down the water column). The agreements are excellent (surface) and good (23 m) in terms of current speed and poor (surface) and reasonable (23 m) in terms of current direction, with the misalignments occurring mostly by low current speeds. Table 8.5 shows the error statistics between the current speed and direction of the model at TNWB and the TNWB data at the observed levels from a depth of 3 m to 36 m. In terms of current speed the agreements vary from excellent (from 3 m down to 22 m) to poor (lower, 36 m level). In terms of current direction the agreements vary between reasonable (from 15 m down to 23 m) and poor (all other levels).
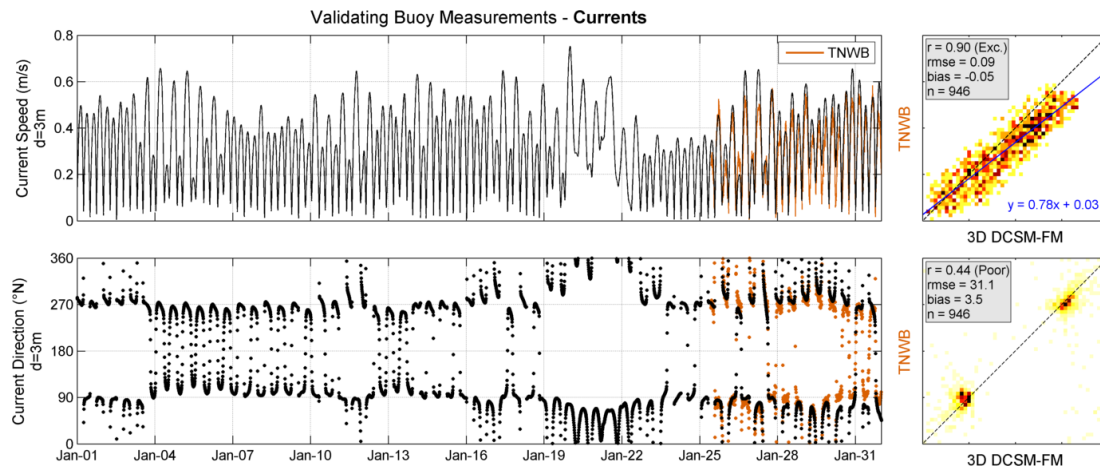
Figure 8.10: *Surface (d = 3 m) current comparison at TNWB (data from January 2021).*

Figure 8.11: *Buoy and 3D DCSM-FM roses (bin width 8°) of the surface (d = 3 m) current velocity at TNWB (data from January 2021). The current direction is the direction the piles point to away from the centre of the rose.*

Figure 8.12: *Current comparison at a depth of 23 m TNWB.*

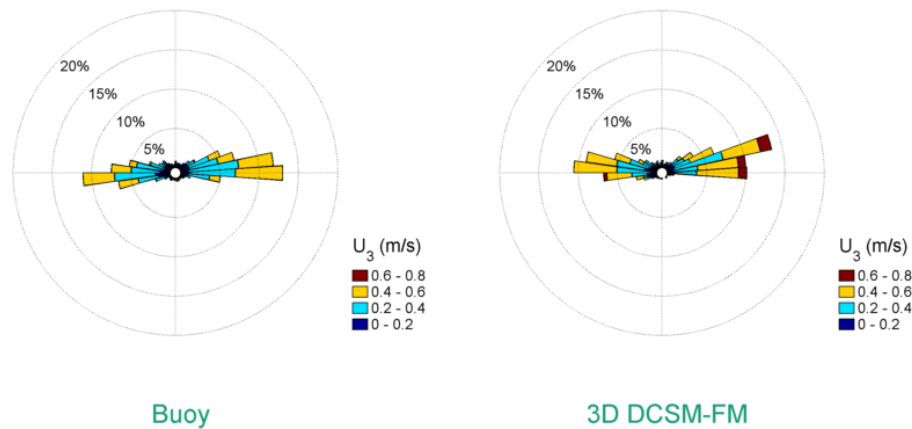TNWB comparison between buoy and 3D DCSM-FM currents (d = 23 m)

Buoy

3D DCSM-FM

Figure 8.13: *Buoy and 3D DCSM-FM roses (bin width 8°) of the 23 m current velocity at TNWB (data from January 2021) The current direction is the direction the piles point to away from the centre of the rose.*
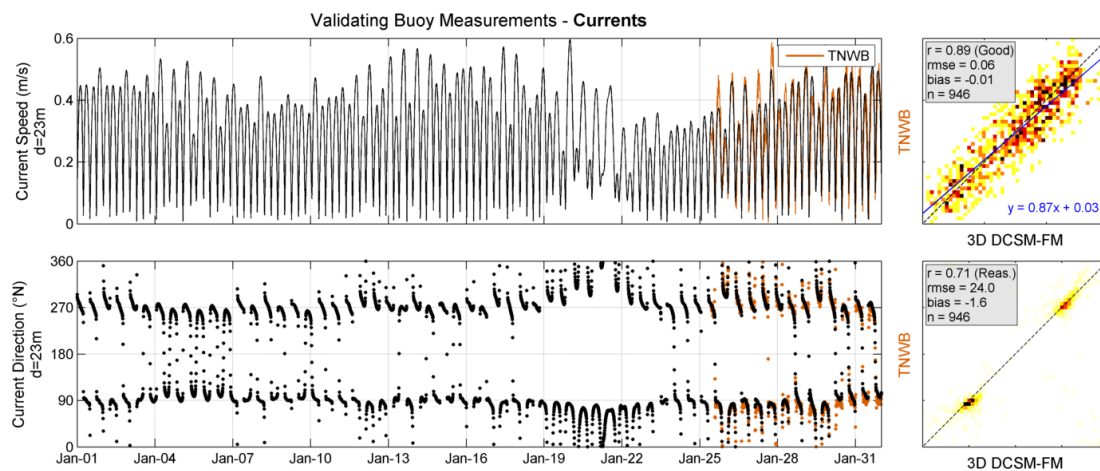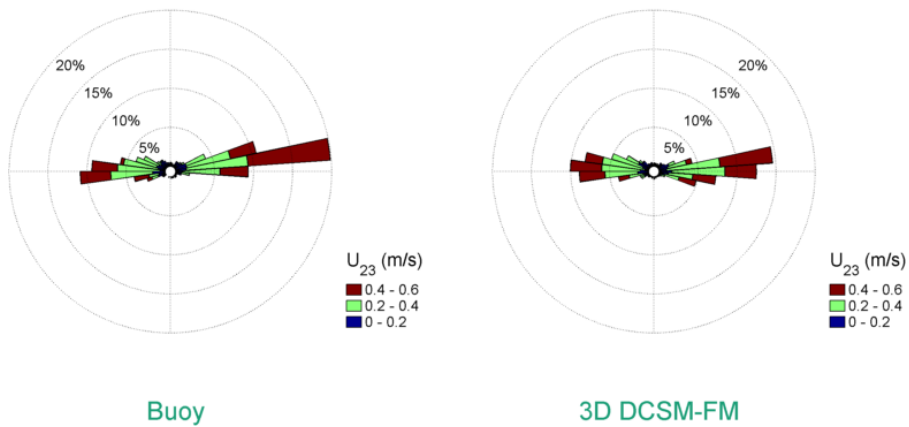
Table 8.5: *Statistical comparison between the 3D DCSM-FM results with TNWB with depth.*

Depth (m)	Current Speed				Current Direction		
	r (-)	Bias (m/s)	Symm. Slope (-)	n (-)	r (-)	Bias (°)	n (-)
3	0.90	-0.05	0.85	946	0.44	3.5	946
4	0.90	-0.04	0.89	945	0.51	1.9	945
5	0.90	-0.03	0.90	946	0.52	2.1	946
6	0.90	-0.03	0.90	946	0.53	0.7	946
7	0.91	-0.03	0.91	946	0.55	0.8	946
8	0.90	-0.03	0.91	946	0.55	0.0	946
9	0.91	-0.03	0.91	946	0.55	-0.2	946
10	0.90	-0.03	0.92	946	0.57	-1.1	946
11	0.91	-0.03	0.92	946	0.58	-1.4	946
12	0.91	-0.02	0.92	946	0.60	-1.8	946
13	0.91	-0.02	0.93	946	0.63	-1.3	946
14	0.91	-0.02	0.94	946	0.68	-1.9	946
15	0.91	-0.02	0.94	946	0.71	-2.0	946
16	0.91	-0.02	0.95	946	0.74	-1.7	946
17	0.91	-0.02	0.95	946	0.74	-2.3	946
18	0.91	-0.01	0.96	946	0.73	-2.4	946
19	0.91	-0.01	0.97	946	0.74	-2.5	946
20	0.91	-0.01	0.97	946	0.74	-2.1	946
21	0.91	-0.01	0.98	946	0.75	-2.5	946
22	0.90	-0.01	0.97	946	0.71	-0.7	946
23	0.89	-0.01	0.98	946	0.71	-1.6	946
24	0.89	-0.01	0.98	946	0.66	-1.1	946
25	0.88	-0.00	0.99	946	0.61	0.3	946
26	0.88	-0.00	0.99	946	0.58	0.2	946
27	0.86	-0.00	1.00	946	0.61	-0.3	946
28	0.86	-0.00	0.99	946	0.64	-0.7	946
29	0.84	0.00	1.01	946	0.63	-0.2	946
30	0.84	-0.00	1.00	946	0.61	-0.0	946
31	0.82	0.00	1.02	946	0.62	-0.4	946
32	0.82	-0.00	1.00	946	0.63	-1.5	946
33	0.80	0.00	1.02	946	0.62	-1.1	946
34	0.80	-0.01	0.98	946	0.64	-2.0	946
35	0.77	-0.02	0.95	946	0.62	-0.8	946
36	0.66	-0.06	0.78	946	0.60	-0.0	946

8.3 Conclusions

As shown above, there is a high agreement between the current speed observations available from TNW and the model results. The obtained low correlations between the current directions are not considered to be due to lack of accuracy in the current direction observations, but model resolution effects and the effect of the nature and variability of the current direction signal on the buoy observations. The found general agreement between the buoy and model data, testify to the quality of both the model results and the observations.

References

EMODnet Bathymetry Consortium, 2016. *EMODnet Digital Bathymetry (DTM),* `http://doi.org/10.12770/c7b53704-999d-4721-b1a3-04ec60c87238`. Tech. rep.

Fisher, N. I., 1993. *Statistical analysis of circular data*. Cambridge Univ. Press.

Fisher, N. I. and A. J. Lee, 1983. "A correlation coefficient for circular data." *Biometrika* 70: 327–332.

IEA Wind, 2017. *"18. FLOATING LIDAR SYSTEMS", IEA Wind Expert group report on recommended practices, 1st edition, September 2017*. Tech. rep.

IEC 61400-12-1, 2017. *IEC 61400-12-1 Wind energy generation systems | Part 12-1: Power performance measurements of electricity producing wind turbines . IEC-TC88 Maintenance Team MT12-1 , Edition 2.0 , 3 March 2017*. Tech. rep.

KNMI, 2009. *HiRLAM version H7.2*. Tech. Rep. `http://projects.knmi.nl/datacentrum/catalogus/catalogus/content/history/HIRLAM72_eng__151009.pdf`, KNMI.

Wieringa, J. and P. Rijkoort, 1983. *Windklimaat van Nederland (in Dutch)*. KNMI (staatsuitgeverij).

Zijl, F. and J. Veenstra, 2018. *Setup and validation of 3D DCSM-FM*. Deltares memo 1220339-005-zks-0003.

Zijl, F., M. Verlaan and H. Gerritsen, 2013. "Improved water-level forecasting for the Northwest European Shelf and North Sea through direct modelling of tide, surge and non-linear interaction." *Ocean Dynamics* 63 (7).

A Hydrodynamic model

3D DCSM-FM covers the northwest European continental shelf, specifically the area between 15°W to 13°E and 43°N to 64°N, and includes the North Sea and adjacent shallow seas and estuaries such as the Wadden Sea and the Eastern and Western Scheldt. It is loosely based on the two-dimensional operational water level forecasting models of the Netherlands (Zijl *et al.* 2013), but uses a flexible mesh with resolution increasing with decreasing water depth (Figure A.1). The smallest cells have a size of 2/3' in east-west direction and 1/2' in north-south direction, which corresponds to 840 m by 930 m in Dutch waters. The optimization methodology is similar to (Zijl *et al.*, 2013), but excludes bathymetry adjustment. The bathymetry is based on a gridded bathymetric dataset (October 2016 version) from the European Marine Observation and Data Network (EMODnet; EMODnet Bathymetry Consortium, 2016) supplemented with survey data for the Dutch coastal zone (cf. Figure A.2)). 3D DCSM-FM uses 20 equidistant sigma-layer in the vertical and includes temperature and salinity as state parameters.
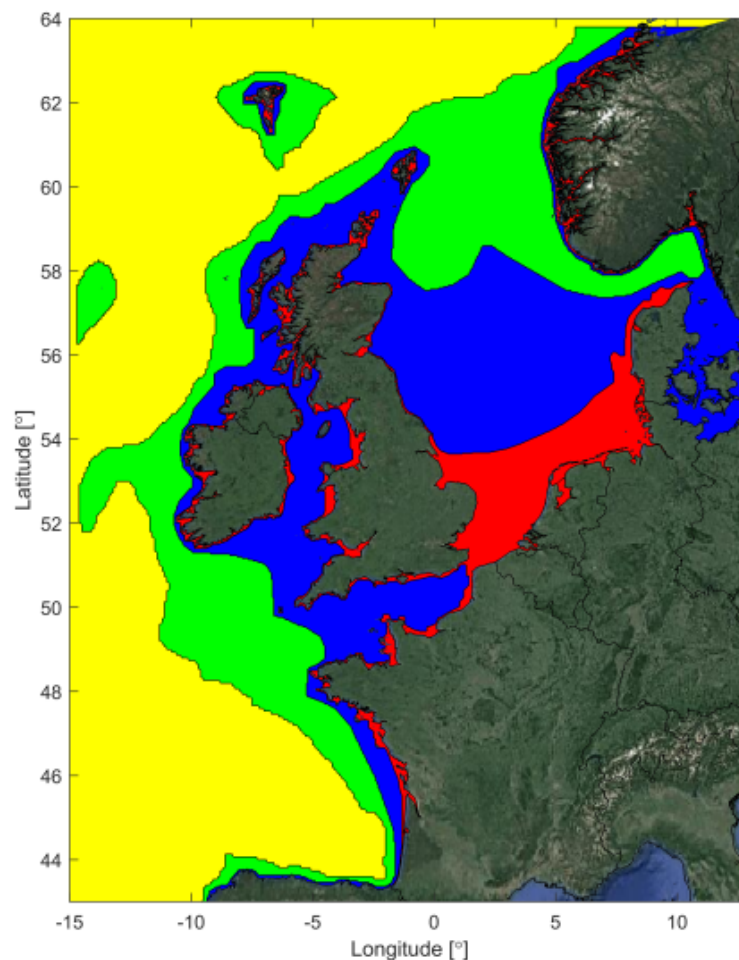

Figure A.1: *Overview of the 3D DCSM-FM model network with the colors indicating the grid size (yellow: ≈ 4 nm; green: ≈ 2 nm; blue: ≈ 1 nm; red: ≈ 0.5 nm).*
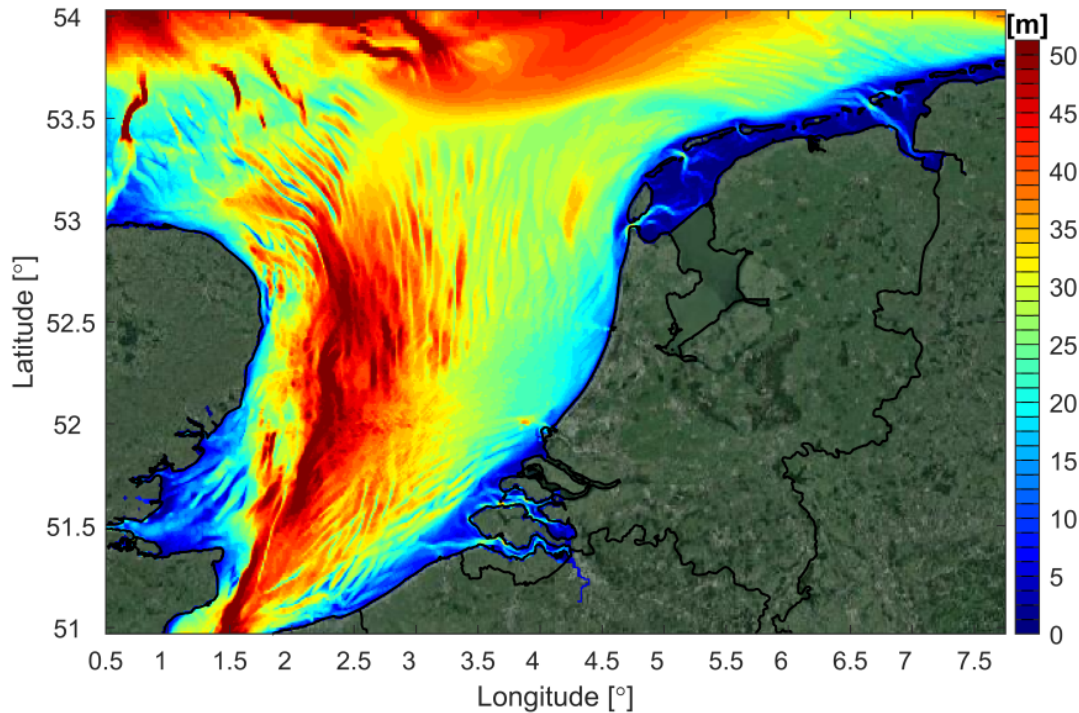
Figure A.2: *3D DCSM-FM model bathymetry in the southern North Sea (depths relative to MSL; source: EMODnet).*

At the lateral open boundaries water levels consisting of a tide and surge component are provided. For the tide 33 harmonic constituents from the global tide model FES2012[1] were used, while for the surge an Inverse Barometer Correction is applied (Zijl *et al.*, 2013). The model includes river discharges, while meteorological forcing in terms of atmospheric wind, mean level pressure, air temperature, cloud cover and dew point temperature are obtained from the KNMI operational Numerical Weather Prediction model Hirlam7.2. (Zijl and Veenstra, 2018) provides further details on the set-up and validation of 3D DCSM-FM .

---

[1]https://www.aviso.altimetry.fr/en/data/products/auxiliary-products/global-tide-fes/description-fes2012.html